*Article*

# A Survey for Recent Techniques and Algorithms of Geolocation and Target Tracking in Wireless and Satellite Systems

Abulasad Elgamoudi * , Hamza Benzerrouk , G. Arul Elango and René Landry, Jr.

École de Technologie Supérieure, 1100 Notre-Dame Street West, Montréal, QC H3C 1K3, Canada; hamza.benzerrouk@lassena.etsmtl.ca (H.B.); ganapathy.elango@lassena.etsmtl.ca (G.A.E.); renejr.landry@etsmtl.ca (R.L.J.)
* Correspondence: abulasad.elgamoudi@lassena.etsmtl.ca

**Abstract:** A single Radio-Frequency Interference (RFI) is a disturbance source of modern wireless systems depending on Global Navigation Satellite Systems (GNSS) and Satellite Communication (SatCom). In particular, significant applications such as aeronautics and satellite communication can be severely affected by intentional and unintentional interference, which are unmitigated. The matter requires finding a radical and effective solution to overcome this problem. The methods used for overcoming the RFI include interference detection, interference classification, interference geolocation, tracking and interference mitigation. RFI source geolocation and tracking methodology gained universal attention from numerous researchers, specialists, and scientists. In the last decade, various conventional techniques and algorithms have been adopted in geolocation and target tracking in civil and military operations. Previous conventional techniques did not address the challenges and demand for novel algorithms. Hence there is a necessity for focussing on the issues associated with this. This survey introduces a review of various conventional geolocation techniques, current orientations, and state-of-the-art techniques and highlights some approaches and algorithms employed in wireless and satellite systems for geolocation and target tracking that may be extremely beneficial. In addition, a comparison between different conventional geolocation techniques has been revealed, and the comparisons between various approaches and algorithms of geolocation and target tracking have been addressed, including $H_\infty$ and Kalman Filtering versions that have been implemented and investigated by authors.

**Keywords:** Radio-Frequency Interference; localization; geolocation; TDOA; FDOA; target tracking; optimization approaches; uncertainty; $H_\infty$ and Kalman filtering

## 1. Introduction

The satellite systems act as relay stations and make up a critical part of the common wireless communications substructure. These systems are employed in most civilian and military implementations, such as the global positioning system (GPS), remote sensing, digital video broadcasting (DVB), high definition video, amateurish radio communications, broadband Internet, weather forecasting, environment surveillance, Global Navigation Systems (GNS), and in several other applications [1–4]. Consequently, the number of Global Navigation Satellite Systems (GNSS) receivers installed on the Unmanned Aerial Vehicles (UAVs) board has increased recently. In general, the aeronautical field is categorized as Manned Aircraft Vehicles (MAVs) and Unmanned Aircraft Vehicles (UAVs). The MAV category requires the presence of a human pilot on the aircraft board, while the UAV category does not require the presence of a human pilot on the aircraft board, and it is controlled remotely over a control room. The number of UAVs, commonly known as drones, has been rapidly increasing in the last decade, and there is an industry analysis that the drone market worldwide will increase by more than 50 billion dollars in 2025 [5]. Based on the market report referred by the GNSS Supervisory Authority (GSA), the number of

drones equipped with GNSS receivers is estimated to be almost 70 million and for other applications, more than twice the number of GNSS receivers required [5,6].

Overcrowding in wireless communication systems may affect these applications and produce Radio Frequency Interference (RFI). The RFI can be classified into two types: unintentional interference, of which over 95% of the satellite communications are suffering, and intentional interference, less than 5% of satellite communication systems are suffering from this kind of interference [7]. RFI may influence these systems, where the source of that interference is required. The RFI sources could be fixed or movable stations on the ground or in the air, such as drones, which are used in military or civilian systems. Figure 1 illustrates the most common interference that may occur in SatCom and GNSS systems.
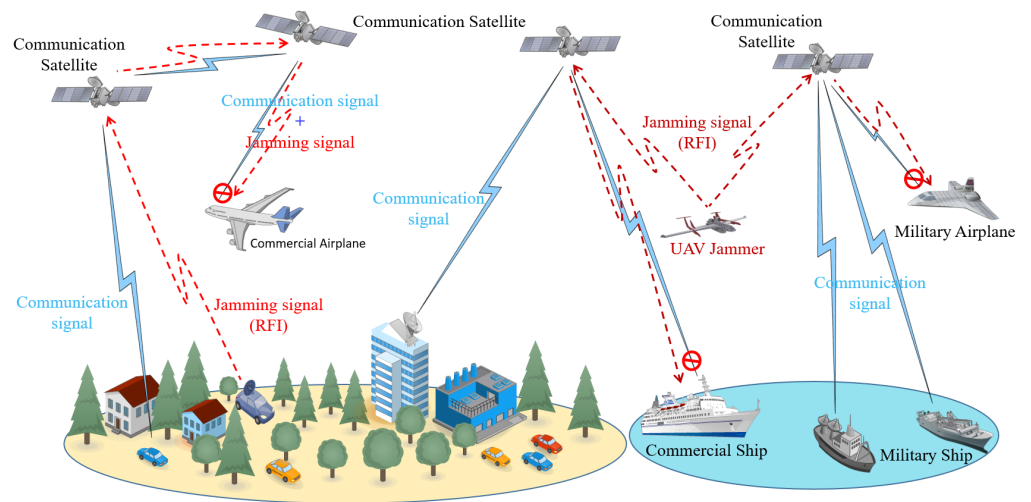


(**a**) Example of interference that may occur in the SatCom system.
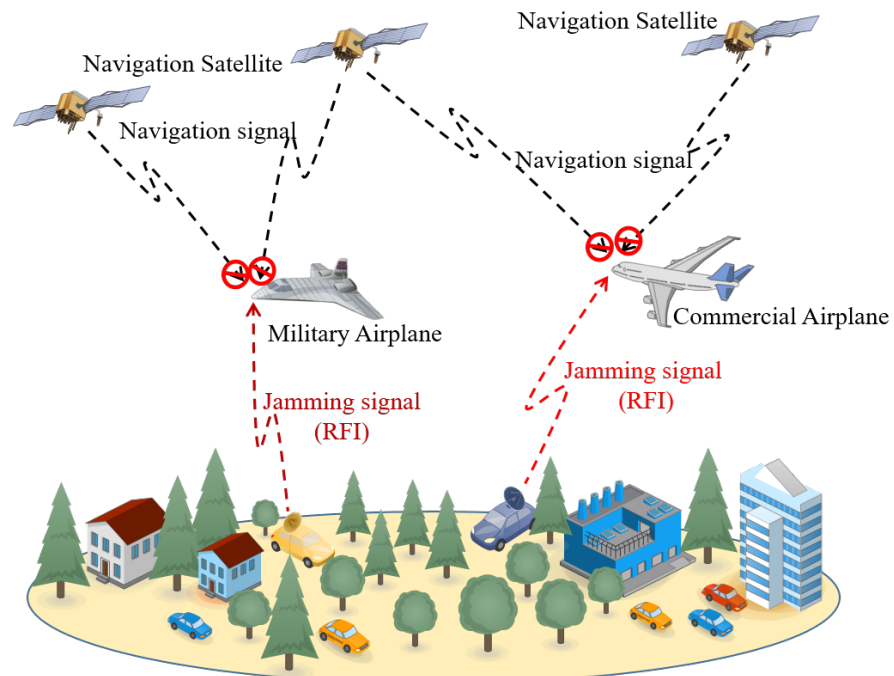


(**b**) Example of interference that may occur in GNSS.

**Figure 1.** Examples of RFI scenarios that may occur in satellite applications.

To secure and protect all wireless and satellite systems from interference or jamming, it is necessary to establish organization for monitoring the wanted signals. The main

two required approaches in this organization are geolocation and emitter tracking. These approaches are required in military and civilian applications, including aerial maneuvers, airspace monitoring, autonomous vehicles, and robots. In addition, these approaches are mainly related to inferring the navigation of an RF emitter, which is assumed to be a random variable, by observing it.

Numerous studies and researches have focused on navigation and positioning issues. Therefore, many useful algorithms have been proposed in the literature [8–11].

The geolocation technique is a measurement making it possible to know if the position of an emitter source is from a fixed station or the initial position of the emitter is dynamic. Various techniques of geolocation measurements can be implemented. For example: Angle of Arrival (AOA), Time of Arrival (TOA), Time Difference of Arrival (TDOA), Received Signal Strength (RSS), Power Difference of Arrival (PDOA), Frequency Difference of Arrival (FDOA), and Differential Doppler Rate (DDR) are the most popular types of measurements. In addition, the accuracy of the emitter geolocation measurement can be improved by combining two or more techniques in one approach, such as hybrid TDOA/FDOA, TDOA/AOA, TDOA/PDOA, and TDOA/FDOA/DDR. Various geolocation measurement techniques and methods have been exhibited in [12,13].

In general, the RF emitter geolocation is not concluded geometrically, but it is estimated by a set of non-linear equations created by the conventional geolocation measurements with the knowledge of the geometry parameters of the sensors used. The optimization approaches for geolocation and target tracking is: (i) A Least Square (LS) and Non-linear Least Square (NLS), (ii) Maximum Likelihood (ML), (iii) Genetic Algorithm (GA) approach, and (v) Constrained Weighted Least Square (CWLS) and Weighted Least Square (WLS) methods [13,14]. Mostly, there are two approaches for solving the non-linear equations: (a) The NLS, which is a direct approach for solving non-linear least squares, or CWLS, which is a constrained framework [15]. (b) An iterative scheme so-called the Taylor series estimation, otherwise known as Gauss–Newton interpolation. This utilizes the solution of a simultaneous set of non-linear algebraic geolocation equations, beginning with an initial guess and updating the guess at each step by finding the local linear least-sum-squared-error correction [16]. Various studies have focused on the ambiguity problem of geolocation methods. For example, the authors of [17] solved the problem of ambiguity for some neighbouring nodes and derived Tangent Linear Approximation (TLA) for the non-linear localization approach, which contributed to incorporating the effect of the neighbours' position ambiguity into Belief Propagation (BP) localization.

Moreover, Kalman Filtering (KF) based on geolocation measurements can be employed to estimate emitter tracking. It is a useful tool for solving navigation and tracking problems. In order to estimate the emitter position, we first must have a reliable estimate of the emitter's present position. Kalman filtering provides a tool to obtain that reliable estimate. It is an algorithm, which uses a form of feedback control. The filter estimates the emitter location. At the same time, it obtains measurement feedback. The KF algorithm operates in two steps. The first step is a prediction: in this step, the filter produces estimates of the current state variables within their uncertainties. The second step is a correction: in this step, the filter will update the measurement using a weighted average, while giving more weight to estimates in higher certainty [18]. Since 1960, several versions of the KF are developed. This filter was improved to be compatible with non-linear systems rather than linear systems, such as the Extended Kalman Filter (EKF), Adaptive Extended Kalman Filter (AEKF), Unscented Kalman Filter (UKF), Cubature Kalman Filter (CKF), and Particle Filter (PF) [19,20].

From the methods and approaches mentioned, it is observed that the current interest in using geolocation and target tracking approaches for RF emitters is increased rapidly. In response to requests imposed by advanced applications that need to geolocate and track the RF emitter at high speeds of movement and rotation, Quadrature Information Kalman Filters (QIKFs) and Gauss–Hermite Quadrature Filter (GHQF), as well as $H_\infty$, have been developed to solve the non-linearity and uncertainty problem [21–24]. To process

such complex algorithms, we have started by introducing a summary of the most popular methods for geolocation and target tracking [12,13,25]. In addition, we have conducted a focused exploration of optimizing-geolocation-measurements approaches, as well as optimal-state-estimation-utilizing-filtering approaches [14–20]. In contrast to the previous studies and surveys, the literature review of this survey focused on the state-of-the-art research articles for geolocation and target tracking approaches for wireless and satellite systems. Table 1 presents recent surveys tackling similar topics for our survey [5,7,26–29]. Based on what was introduced, the main contribution of this survey is presenting the state-of the-art of conventional methods and techniques, compared with more advanced and modern approaches in geolocation and tracking that were developed under uncertainty, biases and coloured noises [21,22,30]. In the end, the original application related to LEO signals of opportunity was also addressed and discussed by providing the readers with several ways to improve the existing methods and solve new problems in theory and practice.

The rest of the paper is organized as follows. Section 2 exhibits the geolocation and target tracking system. Various conventional geolocation techniques have been exhibited in Section 3. In Sections 4 and 5, respectively, past and current approaches of optimizing geolocation measurements and methods of optimal state estimation utilizing filtering have been reviewed. Finally, the conclusions and future works are addressed in Sections 6 and 7.

**Table 1.** Recent surveys tackling similar topics to our survey.

| Survey Ref. | Survey Date | Survey Contribution |
|---|---|---|
| [28] | 2008 | Study various techniques for wireless position estimation. |
| [7] | 2016 | Study positioning systems for wireless systems deploying dynamic sensors. |
| [27] | 2017 | Study solutions of the accuracy and reliability navigation for the 5G positioning system. |
| [29] | 2017 | Study indoor positioning and navigation systems and technologies. |
| [5] | 2019 | Study interference types in GNSS systems, and management solutions of the interference. |
| [26] | 2019 | Study solutions of network design for accurate vehicle localization that have considered the 5G position system. |

## 2. Geolocation and Target Tracking System

The geolocation and target tracking system can be described within five main components as:

i.   The front end equipment for RF signal sensing.
ii.  The geolocation equipment that allows the measurement and determination of the relative position of the RF emitter.
iii. The optimization approaches that allow optimization of geolocation and target tracking algorithms, as well as organizing the non-linear equations within a set of linear equations.
iv.  The optimal state estimation tools, which allow the data smoothing filtering using Kalman filtering.
v.   The display system that allows a display of the position estimation and trajectory of the stationary or mobile RF emitter.

Moreover, consideration must be given to whether the system runs in urban (crowded) areas or rural (open) areas. More details of these components will be exhibited in this survey. Figure 2 illustrates the flow chart of geolocation and target tracking systems.
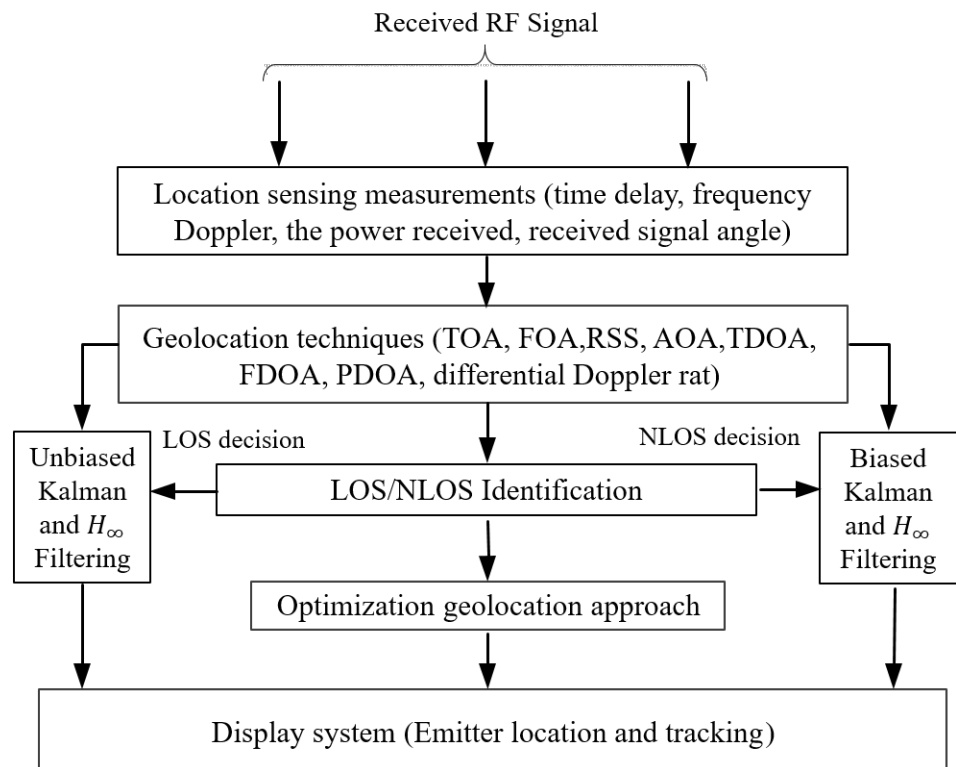
**Figure 2.** Flow of geolocation and target tracking system.

*Urban Environment Characteristics*

In the urban area, the sensors (receivers) may be affected by receiving multi-signals at the same time. This type is called the Non-line of Sight (NLOS) signal. NLOS phenomenon occurs due to the reflection of the original signal when it collides with buildings, towers, and trees [31–33]. Figure 3 presents an NLOS that occurs in the urban environment. During calculation of the geolocation and emitter tracking in the urban area, an NLOS signal should be taken into consideration. For example, if we determine the emitter location as NLOS by TDOA or FDOA measurements, it will be directed to highly bias filtering [34–36].
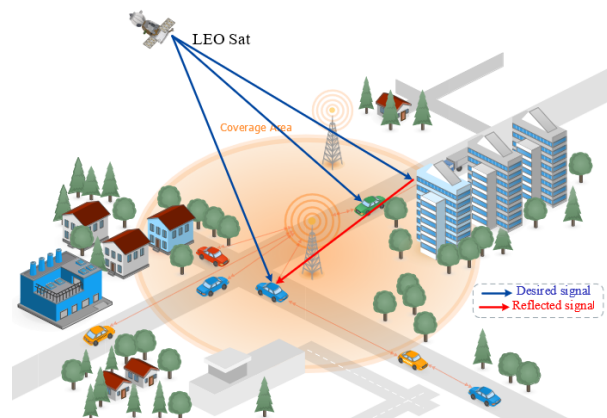


**Figure 3.** NLOS signal reflected from high buildings, towers, or trees.

Geolocation and target tracking algorithms may be affected by NLOS error, which may produce very high errors in geolocation and target estimation. In addition, it may decrease the dependence of the geolocation and target tracking system. To increase the reliability of the geolocation and target tracking system, it should take account of these types of errors [37].

## 3. Conventional Geolocation Techniques

In geolocation techniques, several types of measurements can be employed so that the location can be estimated. In the specified techniques below, we consider the emitter source at a location $p_e = [x, y]^T$, and there, L sensors receive the interference signal from the emitter source, where the location of the sensor is $s_i = [x_i, y_i]^T$.

### 3.1. Angle of Arrival (AOA)

AOA is the angle of the arriving signal at a sensor that was emitted by the target. This angle is utilized to determine the location of the emitter [38].

Based on the direct measurement accuracy ($\pm\theta_s$), the location of the emitter will be determined about the Line of Bearing (LOB) path by $2\theta$ angular spread. A simple triangulation in the AOA technique is used to determine the location of the emitter, as illustrated in Figure 4a. Mathematically, the angle between the emitter and sensor ($i$) is

$$\theta_i = tan^{-1}\left[\frac{(y - y_i)}{(x - x_i)}\right] \tag{1}$$

The authors of [39] have proposed a closed-form solution for geolocation, employing an AOA technique in the presence of sensor position errors; the performance of the algorithm proposed was verified by CRLB and MSE; Figure 4b shows the asymptotic of the proposed algorithm performance to CRLB. The geolocation system can be regarded as that which employs a UAV applying on-board AOA in Line of Sight (LOS) conditions [40]. Employing more than two sensors will produce an increase in geolocation accuracy. When the primary scatter off the radio systems is positioned away from the sensors and located around the emitter, the AOA technique can present a reasonable location accuracy [41]. Yang et al. proposed a weighted AoA-based localization approach; they computed the relationship between the Cumulative Distribution Functions (CDFs) and the localization errors of the three proposed methods with approximate factors, and they have presented a comparison of emitter localization performance based on AOA measurements implemented by two localization scenarios. The first scenario used two-antenna of sensors (L = 2) and the second used three-antenna of sensors (L = 3). From the results achieved, it is feasible that the Least Square Methods (LSM) with a relative factor can minimize the average error by approximately 20% compared to the basic LSM [41]. The AOA technique has some drawbacks, such as complex hardware; in addition, the accuracy and precision decrease when there are signal reflections from adjacent walls or something similar (multi-path), which produces an NLOS error. Therefore, the AOA technique is not suitable as in indoor or urban field geolocation systems [37].
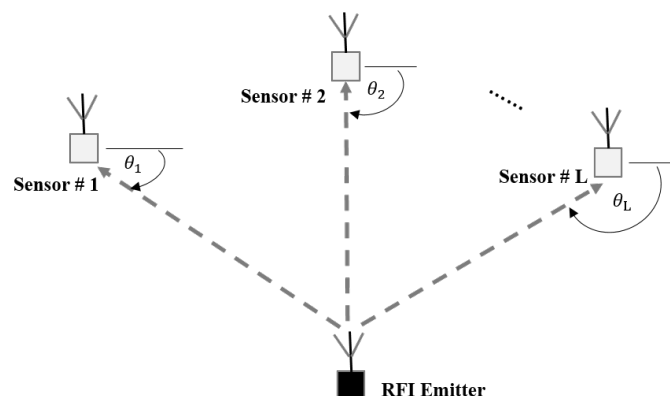


(**a**) AOA geolocation technique with stationary sensors.

**Figure 4.** *Cont.*
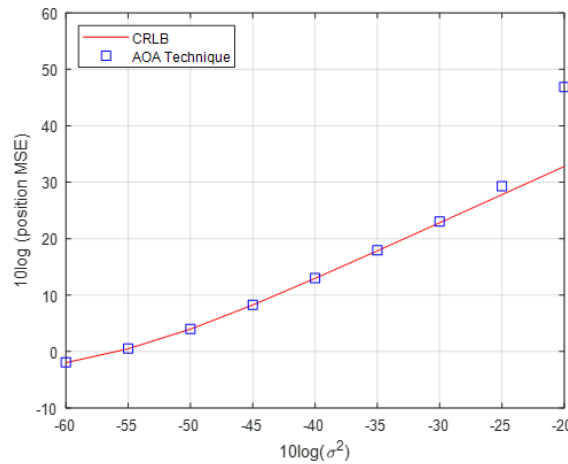
(**b**) Performance verification of the AOA technique.

**Figure 4.** The geometry and Performance validation of the AOA technique. In the simulation scenario, 100 sensor network geometries were considered to achieve the average MSE. The sensors have been divided into 10 groups distributed randomly and centred at $[0, 0, 0]^T$. In addition, the emitter position of each sensor was placed randomly in a larger cube centred at $[0, 0, 0]^T$ with a distance of 500. In addition, the azimuth angle error, elevation angle error and sensor position error were independent [39].

### 3.2. Time of Arrival (TOA)

TOA is the one-way emitting time of the signal propagating between an emitter and a sensor. It means the emitter and all sensors are required to be accurately synchronized to obtain the TOA information. However, such synchronization is not necessary if the two-way of TOA is measured. Each TOA measurement corresponds to a circle centred at a sensor on which the emitter must lie in the 2D space [12,42]. Geometrically, three or more circles were obtained without TOAs noise in a unique intersection, which is the emitter location, indicating that at least three sensors are needed for 2D geolocation, as illustrated in Figure 5.
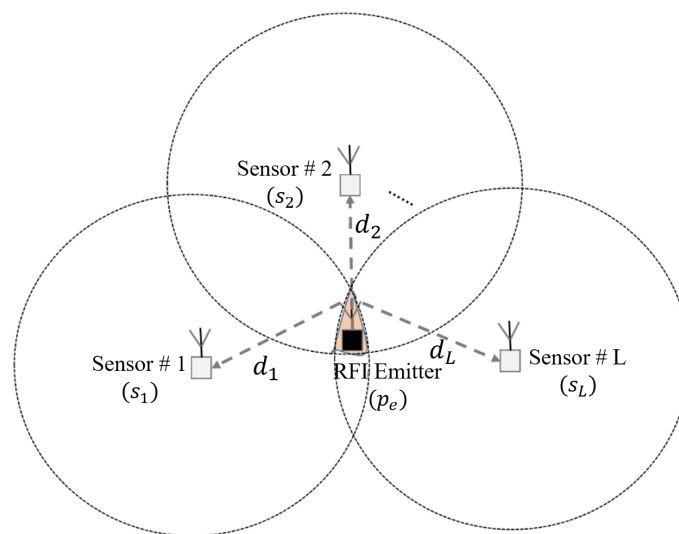


**Figure 5.** Time of arrival geolocation technique.

With the knowledge of three or more sensors, the optimization technique is used to convert the error TOAs measurement into a set of circular equations so that the emitter

location can be determined. Mathematically, the distances between the emitter and sensor (*i*) at a time (t) are calculated as in [43].

$$d_i = p_e - s_i \tag{2}$$

where $p_e$ is the emitter position, $s_i$ is the sensors position and $i = 1, 2, ..L$

From that, TOAs ($\tau_i$) can be calculated by

$$\tau_i = \frac{d_i}{c} \tag{3}$$

where $d_i$ is the distance between the emitter and $i^{th}$ sensors, $c$ is the speed of light at $\approx 2.998 \times 10^8$ m/s.

### 3.3. Time Difference of Arrival (TDOA)

TDOA involves two separate stages of the hyperbolic position estimation. In the first stage, TOA estimation is measured for a signal transmitted between the emitter and sensor (*i*). In the second stage time difference of signal arrive (TDOA) between sensors will be calculated. In this study we considered sensor #1 as a reference. An algorithm is used to estimate the emitter location in the second stage by applying the non-linear hyperbolic equations resulting from the first stage, as illustrated in Figure 6a.
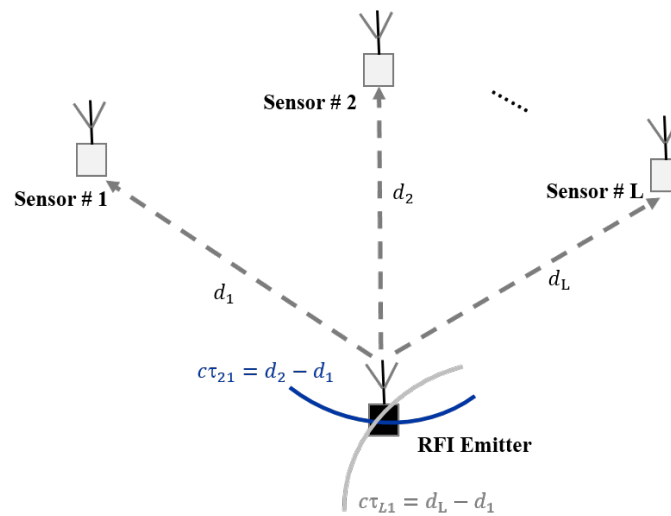
(**a**) The TDOA geolocation technique.
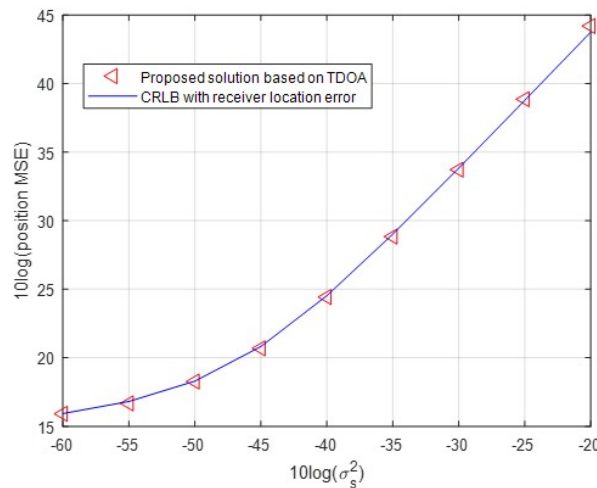


(**b**) Performance verification of the TDOA technique.

**Figure 6.** The geometry of the TDOA measurement and the performance of the proposed algorithm verified by CRLB and MSE. From (**b**), it can be noted that the performance of the proposed algorithm is very asymptotical to CRLB [44].

Mathematically, the TDOA measurement model is formulated as a summation of $\tau_{i1}$, where

$$\tau_{i1} = \frac{(d_i - d_1)}{c}, \qquad i = 2, 3, .., L \tag{4}$$

An important benefit of TDOA is that the processing gain of correlation leads to the enhanced geolocation of signals with suppressed noise even under the receiver noise. In addition, some drawbacks occur in the TDOA method. Firstly, it is hard to achieve synchronization accuracy between all emitters and sensors, in addition to the synchronization error, which can easily translate into 300 meters of range error [36,45].

In [44], six (06) stationary sensors were considered to geolocate a far-field stationary source based on the TDOA technique in the presence of sensor position errors. From the simulation studied, the performance of the proposed algorithm was perfect. In [46], Geometric Dilution of Precision (GDOP) was studied for a multi-station using the TDOA passive localization technique; in this study, precision GDOP with three (03) stationary sensors in a "Y" formation was considered. Various emitter localization scenarios were implemented based on choosing the best sensor distribution. This study concluded that the "Y" formation was the best one for ensuring localization accuracy.

### 3.4. Received Signal Strength (RSS)

RSS is analogous to the TOA technique in which the emitter transmitter must lie in the covering region, the measured distance will determine a circle centred at the receiver. If the power transmitted by the emitter is known, then the distance between the transmitter and the receiver will be calculated to determine the path loss of radio signals through popular mathematical modelling with distances by measuring RSS. Mathematically, the RSS measurement model is the average received power formulated as:

$$p_{r,i} = K_i p_t d_i^{-\alpha} \tag{5}$$

where $p_t$ is the emitter transmitted power in the absence of noise, $d_i$ the distances between the emitter and sensor $i^{th}$, $\alpha$ is the path loss constant, and $K_i$ is other factors that affect the received power. Based on the propagation environment, $\alpha$ is a shift from three to five. Three RSS measurements can calculate the coordinates of the emitter. However, RSS methods also result in significant range estimation errors due to shadow fading effects. Utilizing the pre-measured received signal strength contour centred at the receiver, the accuracy of the RSS methods can be improved by the received signal phase technique [47,48]. Widespread RSS measurements were employed in Wireless Sensor Networks (WSN) based on detection and localization techniques [49,50].

### 3.5. Power Difference of Arrival (PDOA)

The PDOA technique involves the measurement of the RSS of the received signal. It depends on the difference in received signal strength instead of the difference in time of arrival [51–53]. Mathematically, the PDOA measurement model is the received power difference between two sensors formulated as

$$p_{r,i1} = p_{r,i} - p_{r,1} = 10 \, \alpha log_{10}\left(\frac{d_i}{d_1}\right) \tag{6}$$

### 3.6. Frequency Difference of Arrival (FDOA)

FDOA, sometimes called differential Doppler (DD), is a technique similar to the time difference of arrival (TDOA) method. The FDOA is the difference between two Doppler shifts of arrival signals [54–56]. Mathematically, the Doppler shift between the emitter and one of the sensors is defined as

$$\partial f = v\left(\frac{f_0}{c}\right) \tag{7}$$

where $v$ is the velocity (scalar) of closure between the emitter and sensor, $f_0$ is the signal of the carrier frequency, and $c$ is the light speed. FDOA can be expressed as

$$\text{FDOA} = f_{i1} = \partial f_i - \partial f_1 \tag{8}$$

From Figure 7, one can observe how the Doppler shift or FDOA could be extracted from LEO satellite signals of opportunity. In addition, the Doppler rate and Differential Doppler rate can also be extracted or estimated from the carrier phase of the received signal [57].
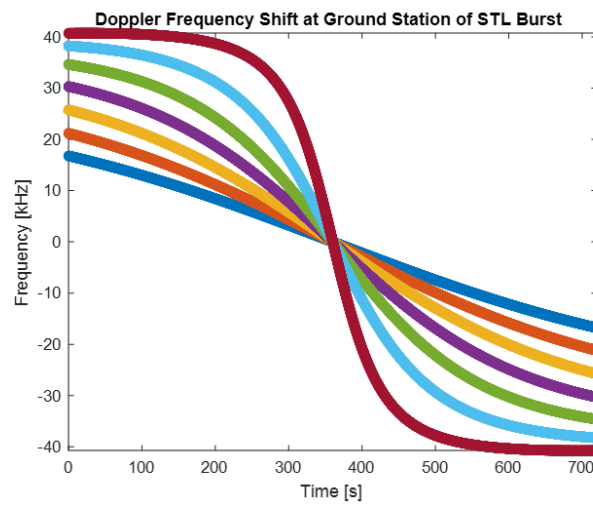
(**a**) Doppler shift estimation
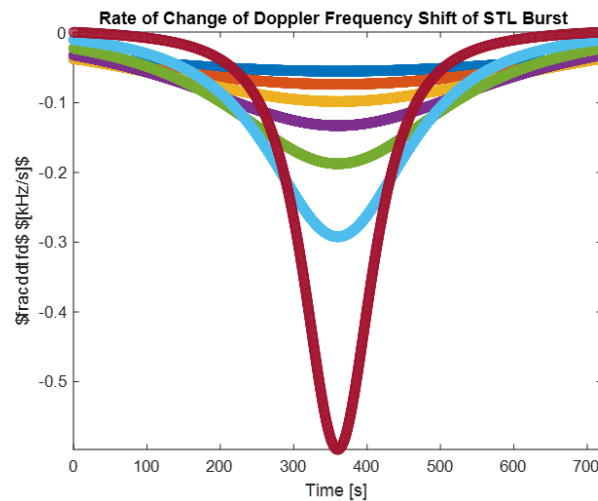


(**b**) Doppler rate estimation

**Figure 7.** FDOA and DDREquivalent Doppler shift and Doppler rate estimation from real LEO satellites downlink signals: Iridium NEXT Simplex signals of opportunity [57].

A critical drawback of FDOA is that significant amounts of data must be moved between observation points to do the cross-correlation processing, which is used to estimate the location of the RFI. In addition, it is very expensive, and it is influenced by the NLOS error [58].

### 3.7. Hybrid Technique of Geolocation Measurements

The hybrid geolocation technique is designed to obtain a more precise estimation of the target's location and reduce the number of sensors needed compared to a particular technique. In the state-of-the-art, various hybrid techniques have been used in geolocation applications, for example, (TDOA/AOA), (TDOA/FDOA), and (TDOA/PDOA) [59–63].

### 3.7.1. TDOA/AOA

The hybrid TDOA/AOA measurement model combines the TDOA measurement with the AOA measurement between sensors, as illustrated in Figure 8a.
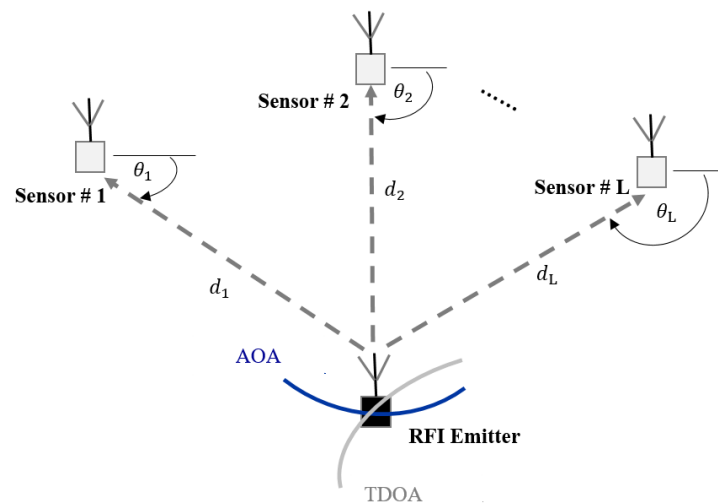
(**a**) Geometry of the hybrid TDOA/AOA technique.
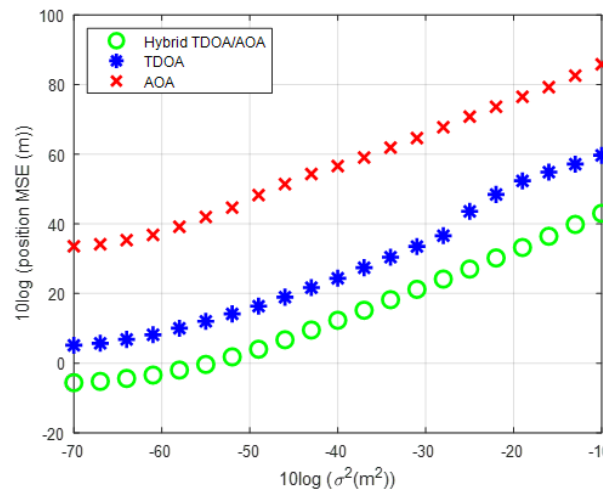


(**b**) MSE comparison between TDOA, AOA, and the hybrid (TDOA/AOA) technique.

**Figure 8.** The geometry and performance verification of the hybrid TDOA/AOA technique. Individual comparisons of the performance scenario of the hybrid TDOA/AOA technique with TDOA and AOA techniques was the main object in this scenario. Authors' own elaboration.

Mathematically, the hybrid TDOA/AOA measurement model is formulated as:

$$TDOA/AOA = [\tau^T, \theta^T]^T \tag{9}$$

where $\tau = [\tau_{21}, \tau_{31}, \cdots \tau_{L1}]^T$ and $\theta = [\theta_1, \theta_2, \cdots \theta_L]^T$ were derived in [64], where E-Systems have utilized hybrid TDOA/AOA measurements for the Cellular Applied to IVHS Tracking and Location (CAPITAL) Beltway Project [65,66]. The capital system can geolocate the target mobile by monitoring the reverse link voice channel transmitted by the mobile user at the base station. Multiple base stations receive the signal, and the target position is determined by combining AOA estimates from each base station and TDOA estimates between multiple base stations [67,68]. The arrival time of a signal is measured at each base station that is time-stamped with a GPS reference time to estimate the time reference of arrival estimates. The spatial filtering offered by the highly directional antennas is used for minimizing the impact of the multi-path [69].

Mohammad et al. proved that hybrid TDOA/AOA is a more accurate and has the best performance compared to TDOA and AOA individually. In this study, a two-step LS algorithm based on TDOA, AOA and a hybrid TDOA/AOA were applied to optimize

geolocation measurements for mobile emitter using multi-sensors. Root-Mean Square Error (RMSE) against Signal to the Noise ratio (SNR) was computed in this simulation [68].
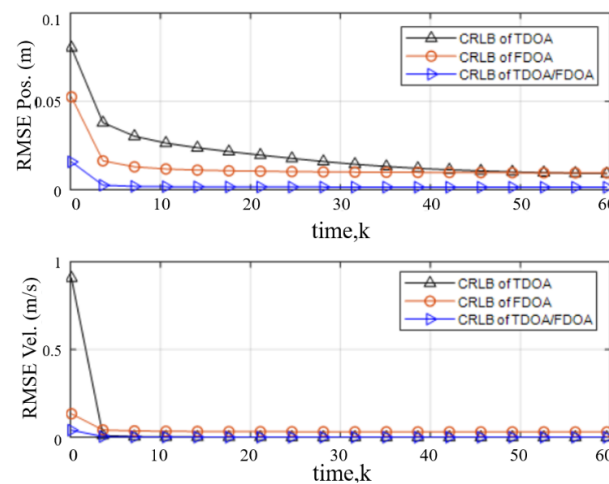
### 3.7.2. TDOA/FDOA

This technique is a combination of FDOA and TDOA measurements. Employing this measurement can increase the accuracy of geolocation and reduce the number of sensors needed. The Newton–Raphson method is the most common method used as the geolocation engine to solve this over-constrained problem [70,71].

Abulasad et al. demonstrated that the hybrid TDOA/FDOA measurement is more precise and better-performing compared to TDOA and FDOA measurements individually, which utilize three sensors. Figure 9a shows the geometry of the geolocation technique based on the TDOA and FDOA measurements. Figure 9b shows the CRLB comparison between TDOA, FDOA, and the hybrid (TDOA/FDOA) measurements [21].
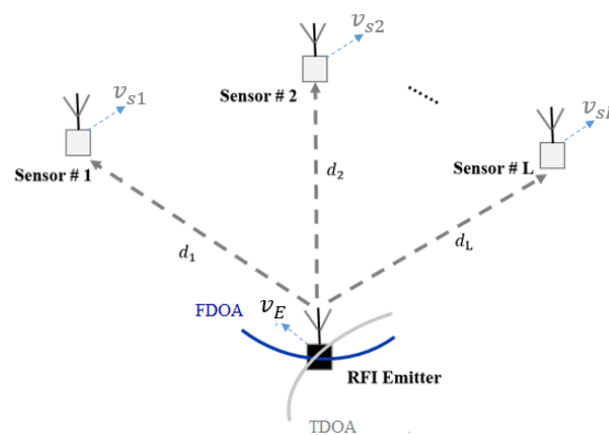


(**a**) Geometry of the hybrid TDOA/TDOA.



(**b**) CRLB comparison between TDOA, FDOA, and the hybrid (TDOA/FDOA)

**Figure 9.** The geometry and Performance verification of hybrid TDOA/FDOA measurements compared to TDOA and FDOA individually [21].

The cross ambiguity function (CAF) is used to determine the time of the emitted signal of TDOA and FDOA using at least two sensors. The CAF measurement is applied, and the surface is formed based upon functional offsets. From the CAF function, the dominant peak value formed on the surface determines the real computed values of TDOA/FDOA integrated into signals ($signal_1$, $signal_2$) and maps these values with the CAF magnitude by means of sensor and emitter geometries [72].

Figure 10a shows the geometry of the TDOA/FDOA geolocation measurement in terms of CAF. Mathematically, CAF can be formulated as

$$\mathrm{CAF}(\tau, f) = \sum_{N=1}^{n-1} sig_1[n]sig_2^*[n + \tau]e^{\frac{-j2\pi fn}{F_s}} \tag{10}$$

where $\tau$ and $f$ are time and frequency of arrival, $sig_1[n]$ and $sig_2[n]$ are analytic signals received at sensor #1 and sensor #2, the $(*)$ denotes a complex conjugate, $F_s$ is the sampling frequency of the collected signals [72,73].
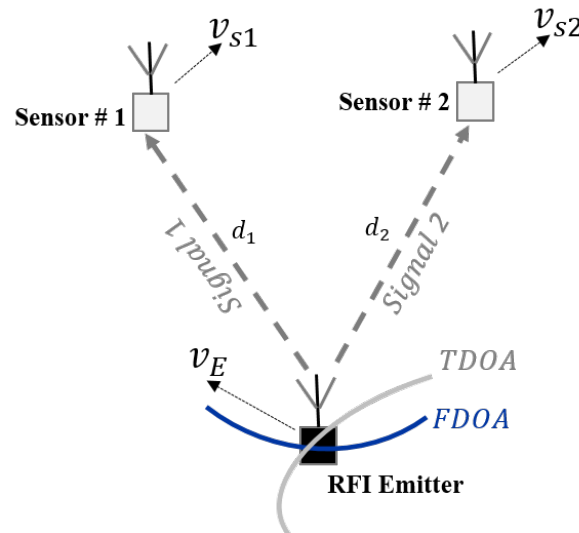


(**a**) Geometry of the TDOA/FDOA measurements based on the CAF technique.
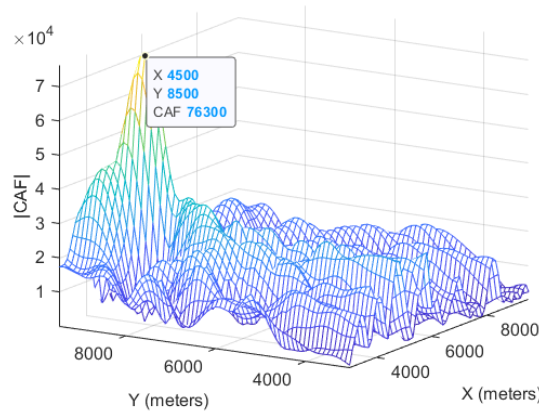


(**b**) CAF peak for estimating the emitter geolocation.

**Figure 10.** Pair of moving sensors were considered to geolocate a static RFI emitter using the CAF method. The simulation result achieved the peak of CAF that denotes an estimated RFI emitter position. Authors' own elaboration.

### 3.8. Tri-Combination Technique of Geolocation Measurements

More than two conventional positioning measurements can be combined to achieve a more precise estimate of the target's location. There are various applications; each one uses a selected scheme, which depends on the geolocation environment and type of application needed. Demonstrations of a tri-combination of geolocation measurement can be found in several applications, such as TDOA/FDOA/DFS [74], TDOA, FDOA, and differential Doppler rate [75], and TDOA, FDOA and Doppler Rate [76].

The improvement in the emitter geolocation method using the Tri-combination of geolocation measurements was the authors' own elaboration, and they compare it to a hybrid measurement, which was achieved in [21]. Figure 11 illustrates the CRLB verification for combining TDOA/FDOA/DDR and comparing it with the hybrid TDOA/FDOA as well as TDOA and FDOA individually.



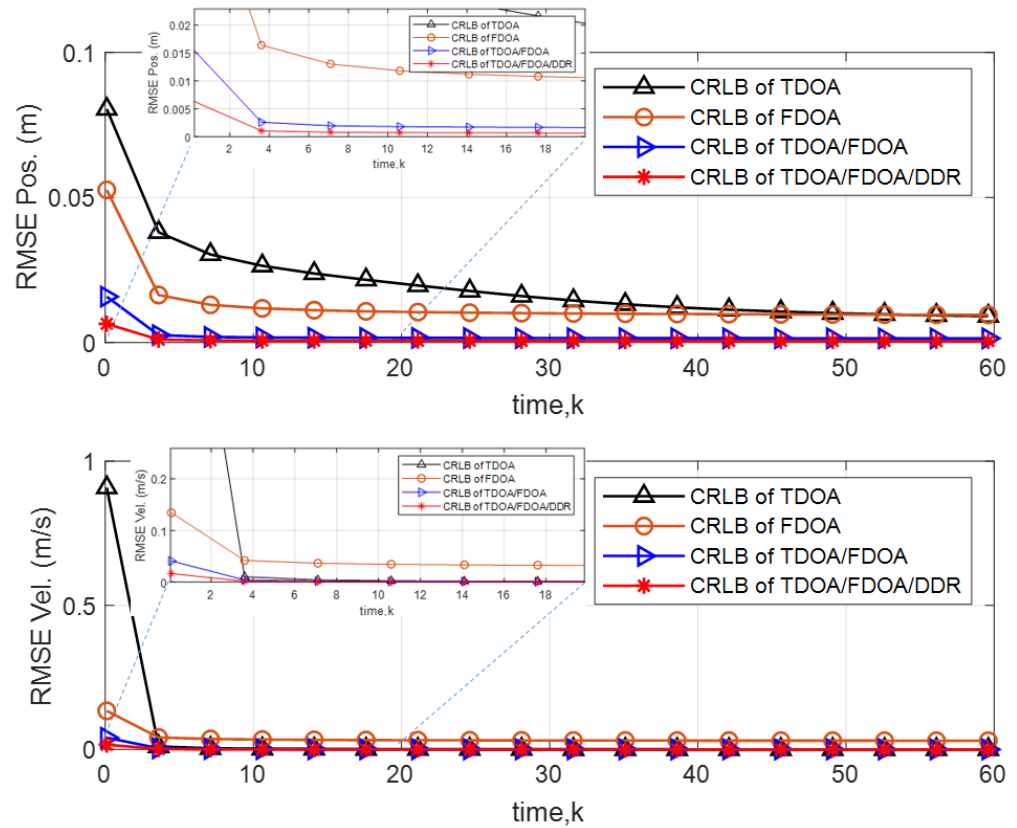**Figure 11.** CRLB comparison between TDOA, FDOA, hybrid (TDOA/FDOA), and Tri-combination of (TDOA/FDOA/DDR). In this figure, the same scenario and input parameter has been implemented in Figure 9b. Additionally, TDOA/FDOA/DDR was computed and its performance compared. Authors' own elaboration.

Table 2 shows the review of a comparison between different types of measurements used for conventional geolocation.

**Table 2.** Comparison between numerous conventional geolocation techniques.

| Technique | Signal Measurement | Advantages | Drawbacks |
|---|---|---|---|
| AOA | Direction angle | No need to time-synchronize, and two sensors minimum are required [77,78]. | Need a complicated and expensive antenna; the accuracy of geolocation is decreasing at far-field [66,79]. |
| TOA | Time delay | Accurate [77,80]. | Need synchronization between all sensors, affected by NLOS errors, and more than two sensors are needed, it is complex hardware [80]. |
| TDOA | Time difference | No need for synchronization between all sensors, the accuracy approximately the same in the near field and far-field [78,79]. | More than two sensors are needed and affected by NLOS errors [80]. |
| RSS | Power signal | Cheap and simple, and no need for synchronization between all sensors [80]. | Inaccurate, the reliable distance estimation is required to achieve an accurate propagation model, more than two sensors are needed, as well as it is affected by NLOS error and shadowing [80]. |
| PDOA | Power difference | Better than TDOA, splashily in urban area [51]. | Inaccurate in an open area compared to TDOA [51]. |
| FDOA | Frequency difference | No need to know the carrier frequency previously [58]. | It is very costly, and it affected by NLOS error [58]. |
| AOA/ TDOA | Angle and Time difference | Fewer sensors are needed, more accurate [78–80]. | Complex hardware, LOS assumed [80]. |
| TDOA/ FDOA | Time and Frequency difference | High accuracy spatially with moving sensors and emitter [80]. | Difficulty in determining the accuracy of non-linearity sensors location and velocity [81]. |
| TDOA/ FDOA/ D.Rate | Time, Frequency, and Doppler Rate difference | Superior performance achieved [75]. | Complicated method [75]. |

## 4. Approaches of Optimizing Geolocation Measurements

In this section, we review previous and state-of-the-art geolocation and target tracking approaches that deal with wireless and satellite applications employing different geolocation measurements.

### 4.1. Taylor Series (TS)

The Taylor Series (TS) is an infinite sum of values, which is expressed in the function's derivatives at a single point. This function uses the least square method to estimate the initial coordinates of a target location.

In [82], a Taylor Series algorithm based on the Semi-Definite Programming (SDP) method was employed. Moreover, the squared distance difference model was implemented to obtain a rough location of the target node. After that, the geolocation of the target node was formulated as a linear least square problem using the Taylor Series expansion; they applied a localization simulation for emitter and sensors geometry, as illustrated in Figure 12. Improving the positioning accuracy using the Taylor series algorithm based on the TDOA measurement was proposed in this study. In the simulation scenario, eight anchor nodes and one target node with coordinates were considered to localize the target node. The performance of the proposed algorithm was compared with semi-definite programming (SDP) and CRLB, and the Taylor Series algorithm for localization was exam-

ined and compared with the semi-definite programming method for emitter coordinates $\{35, 35\}$ m.
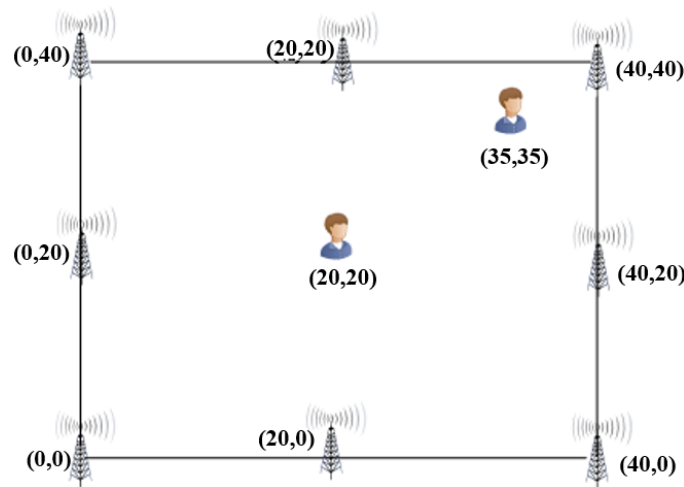


**Figure 12.** Distribution of sensors and emitter scenario [82].

The Taylor Series expansion based on a new localization algorithm was proposed by the author of [83] for the NLOS environment. The algorithms such as Radial-Basis-Function (RBF) and Taylor (Least Square) LS-Taylor have achieved better performance as compared to other algorithms in the NLOS environment.

### 4.2. Maximum Likelihood Estimator (MLE)

Maximum Likelihood Estimator (MLE) is an approach for estimating the probability distribution parameters by maximizing a likelihood function. The maximum point of the parameter space is called the maximum likelihood estimate [84].

In [85], the problem of multi-static sonar with a transmitter has been addressed. Two solutions based on TOA and AOA measurements to estimate the object were proposed in that study. In addition, the localization parameters were updated by MLE, and an approach, as well as precise propagation speed, can be obtained from MLE proposed. Figure 13 illustrates the geometry of sonars, the transmitter, and the object. The simulation results exhibited that the proposed algorithm can produce the optimal solution to the MLE problem. Furthermore, an accurate localization solution and propagation speed update was achieved using RMSE and CRLB.
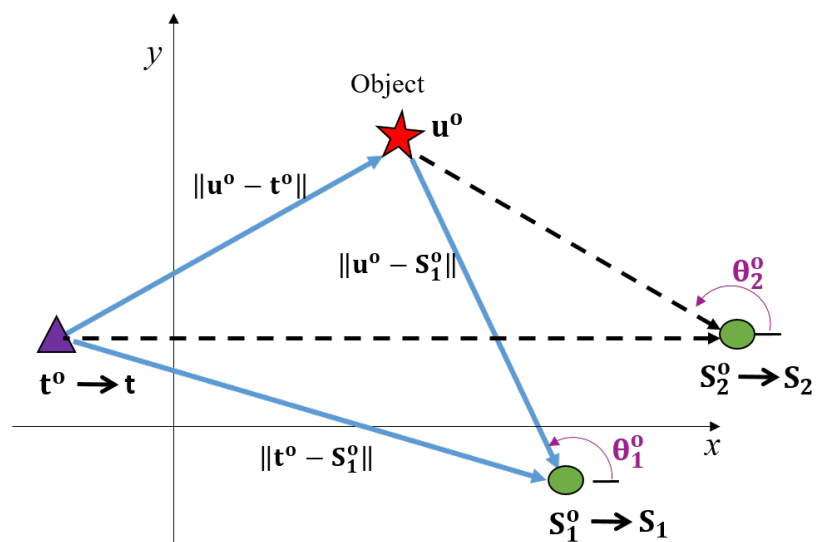


**Figure 13.** Scenario of multi-static sonar, a transmitter, and the object [85].

### 4.3. Least Square (LS)

The Least-Squares (LS) approach is a standard method that may be used to optimize emitter localization measurements. The method depends on minimizing the amount of the squares of the residuals obtained in the results of all individual equations [86]. In [87], the geolocation scenario and performance of the proposed algorithm was validated using Linear Least Squares (LLS). In this scenario, four static sensors were considered to geolocate a moving target using the LLS method based on the TOA/RSS measurement, as shown in Figure 14. The mean square position error (MSPE) against the Signal to the Noise ratio (SNR) was computed in this scenario to present the performance of the proposed algorithm.
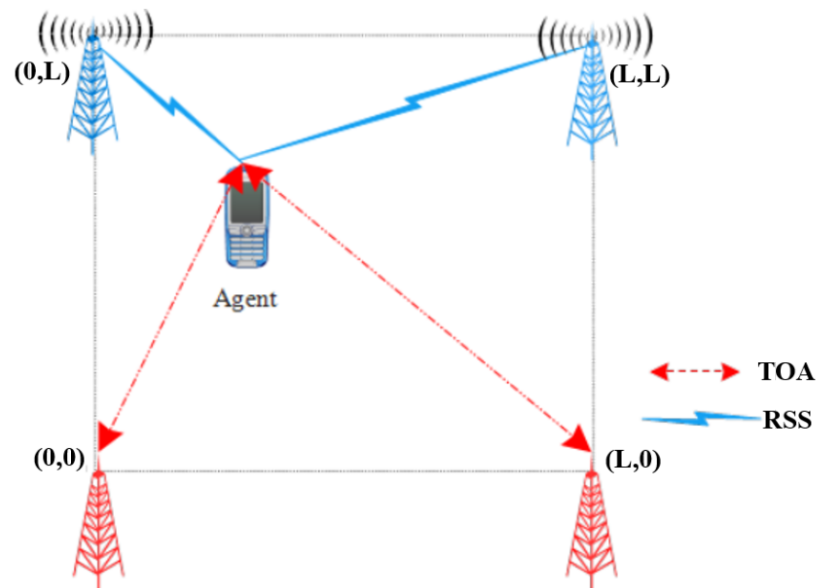


**Figure 14.** Distribution of the sensors and emitter for the proposed scenario [87].

A Non-Linear Least Squares (NLLS) estimator can be utilized to solve non-linear functions that cannot be solved analytically. Consequently, numerical search algorithms such as the Newton and the Gauss–Raphson algorithms are utilized to approximate the NLS estimate. Moreover, the LLS algorithms can be employed in the non-linear expressions to obtain a closed-form solution and avoid the explicit minimization problems [77,88].

### 4.4. Weighted Least Square (WLS)

The weighted least squares (WLS) is defined as an ordinary least squares and linear slope in that the error covariance matrix is allowed to be different from a status matrix. This approach has been commonly used in numerous geolocations and target tracking scenarios recently. For example, in [89], the WLS algorithm was proposed for estimating the position target employing the hybrid RSS/AOA measurements of the signals received at several sensors. In an explicit manner, in the proposed algorithms, the source location coordinates with known relation between the intermediate variable and the source location coordinates are an advantage. By using 2nd order Taylor approximation assuming perfect knowledge of the actual target location, the author derived an approximate error covariance matrix under Gaussian measurement noise. The least-squares solution is considered for computing the relative error of the covariance matrix without knowledge of the target location under measurement noise over the sensor nodes instead of the true target position. The superiority of the proposed algorithm when compared to the LS algorithm confirms the minimum estimation bias and Root Mean Square Error (RMSE) for estimating the position of the emitter source. Figure 15 illustrates the geometry of the proposed scenario.
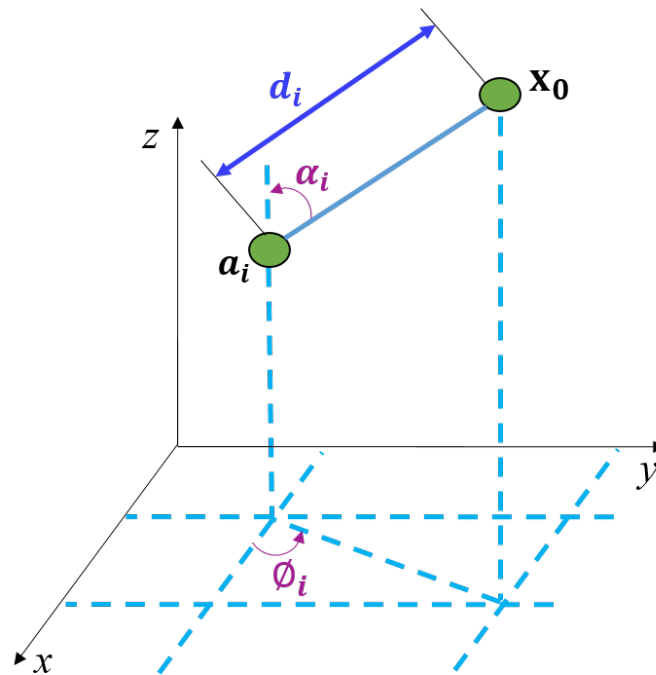
**Figure 15.** Geometry of the sensor and target location in 3D [89].

Wang et al. proposed a practical iterative constrained weighted least squares (ICWLS) algorithm to estimate multiple targets by multiple mobile sensors and multiple calibrations, as shown in Figure 16, which used TDOA/FDOA localization measurements. The proposed method consisted of two stages. In the first stage, the location of the sensors is enhanced based on the calibration measurements as well as the previous knowledge of the sensors position. In the second stage, the estimate of the multiple target geolocation is obtained by joining the measurements of emitted signals and the estimated values obtained in the first stage [90]. The simulation results demonstrated that the proposed algorithm could produce the optimal solution to the formulated constrained WLS problem. Additionally, its estimation RMSE can achieve CRLB with calibration emitters at common noise; from that, the analytical validation results verified that the proposed algorithm is better than some existing localization algorithms [90].



**Figure 16.** Multi-sensors, multi-emitter calibration, and multi-agent geometry [90].

In [91], a simple algorithm is designed for movable target estimation using three or more stationary sensors. The performance of the proposed algorithm was verified by CRLB and compared with the LLS, quadratic least squares (QLS) and two-step WLS algorithms.

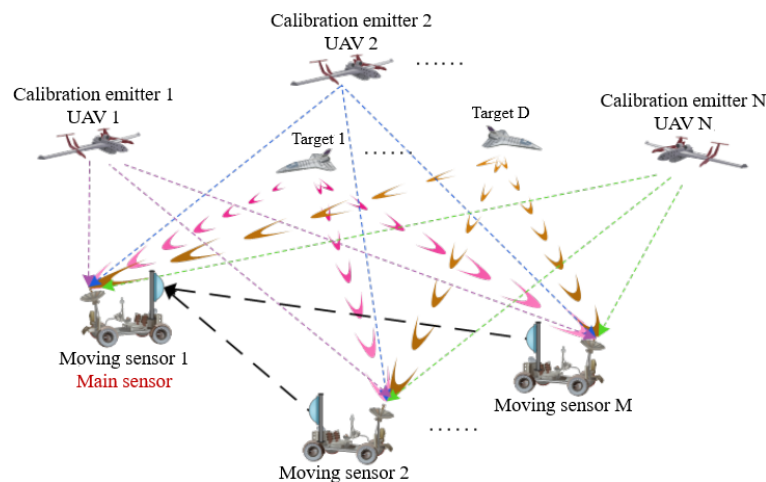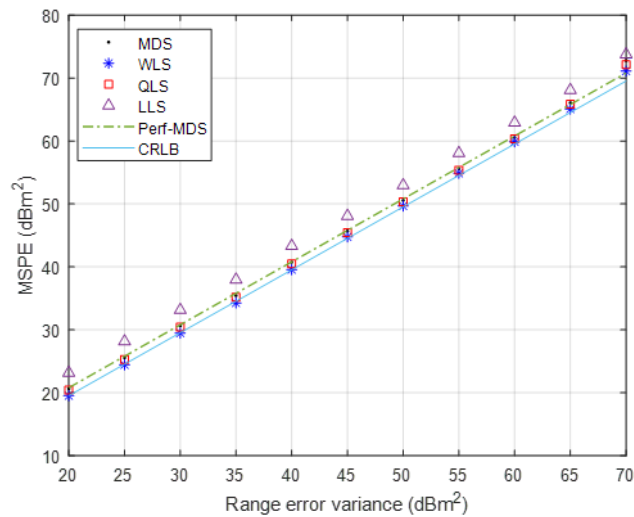In this study, the corresponding mean relative position errors (MRPEs) and the mean square position errors (MSPEs) versus range error variance, ignoring multi-path and NLOS errors, were computed and simulated, as shown in Figure 17.



(**a**) Mean Square Position Error.
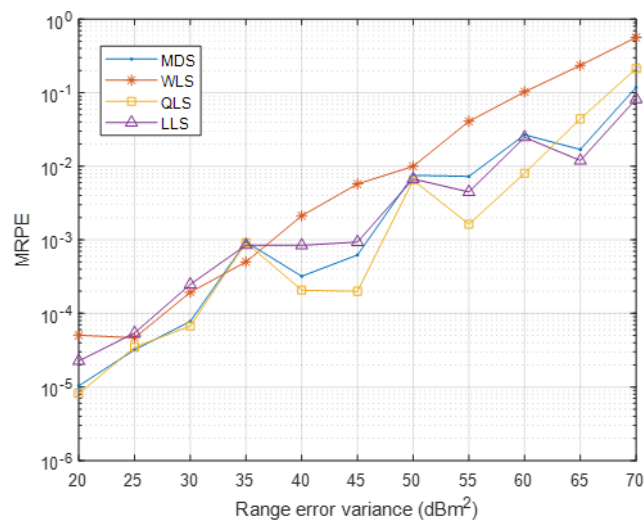


(**b**) Mean Relative Position Errors.

**Figure 17.** Algorithm performance comparison (MSPE and MRPE for three-BS geometry without NLOS). From the figures, it can be noticed that the two-step WLS algorithm has the best performance compared to other methods [91].

In [75], an algebraic method for the estimation of the location and velocity of a moving source using TDOA, FDOA, and differential Doppler rate measurements of a signal received at several sensors with sensor location errors were proposed. The method depends on the two-step weighted least square estimator and the pseudo-linear set of equations. In the algorithm, the tri-combination of the geolocation measurement was proposed. The estimated precision of the emitter position and velocity is displayed to achieve the Cramér–Rao lower bound (CRLB) for Gaussian TDOA, FDOA, and differential Doppler rate noise at a measured noise level before the thresholding effect occurs.

### 4.5. Artificial Intelligence (AI)

Artificial intelligence (AI) is a group of many different technologies working together to achieve the desired goal. It is implemented in control and communication systems,

as well as employed in geolocation and emitter tracking estimation. For example, the Genetic Algorithm (GA) approach is used to optimize classical geolocation measurements, and Dempster–Shafer (D-S) theory is used to optimize target tracking estimation [92,93].

It is important to mention that there are open public datasets of RF signals in the format that contains I and Q at different sampling rates. The best example one can find is the following datasets and platform: RF datasets for machine learning, see [94]. However, this dataset is mainly dedicated to signals classification and not geolocation and positioning; nevertheless, it is still interesting to investigate if one can estimate and extract navigation data (Doppler shift, Doppler rate) from raw data.

### 4.5.1. Genetic Algorithm (GA)

In the geolocation field, Genetic Algorithms (GA) have been developed to overcome the drawbacks of geolocation algorithms in traditional methods. In the early 1970s, John Holland introduced the concept of GA. There are two requirements to define a typical genetic: a genetic representation and fitness function; (i) A genetic representation of the solution domain, and (ii) a fitness function to evaluate the solution domain. GA can be represented by a sequence of procedural steps for moving from one population of chromosomes (by artificial intelligence) to a new population. Each chromosome consists of some genes. Each gene may be represented by binary strings, real numbers, permutations of an element, or a program element (genetic programming) [92]. In [95], for the first time, the authors implemented a GA based on TDOA measurements in Taiwan. They achieved noted improvement in the accuracy of geolocation. This study considered five monitoring stations distributed in 3D as A = (0 km, 0 km, 0 m), B = (10 km, 10 km, 100 m), C = (10 km, 10 km, 100 m), D = (0 km, 10 km, 100 m), and E = (10 km, 0 km, 0 m) . The experiment result showed that the measurement error decreased when the number of monitoring stations increased. When the NLOS is considered, the results showed that the geolocation accuracy at a circular error probability of 50% was less than 60 m. Moreover, the proposed algorithm yielded 17-fold and 19-fold improvement when the emitter location was favourable and unfavourable compared to the hyperbolic calculations based on conventional TDOA measurements.

### 4.5.2. Dempster–Shafer (D-S)

Dempster's work on the theory of probabilities with upper and lower limits gave rise to the Dempster–Shafer (D-S) theory of proof. It has since been expanded by a number of researchers and popularised in the literature on AI and expert systems, but only to a limited extent, as a technique for modelling reasoning under uncertainty. In this regard, it has a number of advantages over more traditional statistical and Bayesian decision-making methods. Hajek remarked that actual, functional applications of D-S methods have been uncommon, but subsequent to these remarks, there has been a marked increase in the applications integrating the use of D-S. Although D-S is not widely used, it has been successfully applied to target identification and target tracking [93].

In [96], the authors have made a comparison between D-S and Bayes theories. They have derived the KF from the basic Bayesian fusion equation using a new method to estimate the Chapman–Kolmogorov prediction integral. Eventually, they concluded that the D-S theory is better than Bayes theory.

A multi LEO satellite was considered to geolocate and track the UAV using D-S to optimize high non-linear filtering. Various simulation scenarios were implemented with Continuous-Discrete Gauss Hermite $H_\infty$ filtering (C-DGH$H_\infty$F) in the presence of uncertainty, as shown in Figure 18.
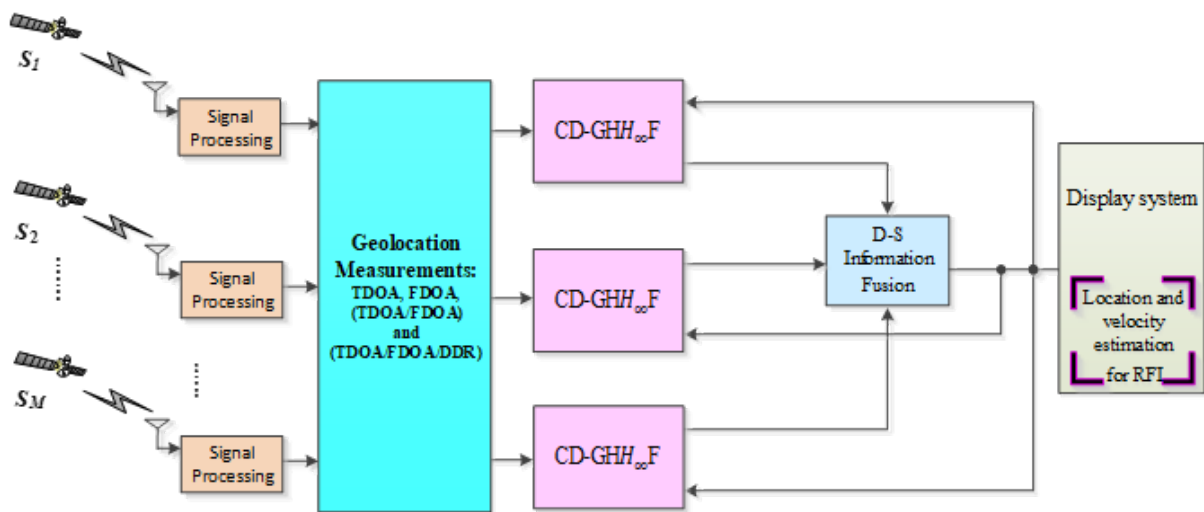
(**a**) The schema for RFI tracking and geolocation using Dempster–Shafer (D-S) theory.
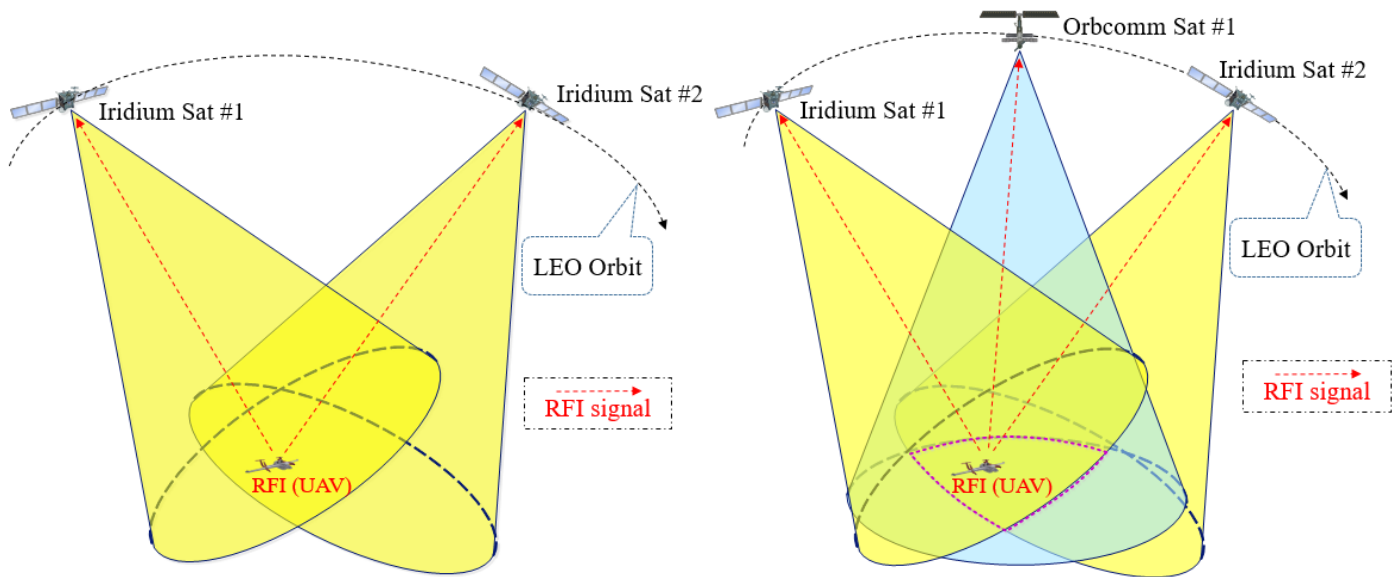


(**b**) 02 LEO Iridium Sat tracking UAV jammer,



(**c**) 02 LEO Iridium Sat and 01 Orbcomm Sat tracking UAV jammer.

**Figure 18.** Various scenarios of RFI UAV tracking based on TDOA/FDOA/DDR using Iridium and Orbcomm Sat. in VHF-L band. Authors' own elaboration.

### 4.5.3. Machine Learning (ML) and Deep Learning (DL) Approaches

Machine Learning (ML) and Deep Learning (DL) methods are based on AI networks and GA with representation learning. This learning may be under supervision, semi-supervised or unsupervised [97–99].

The authors of [100] presented a position estimate approach based on deep learning algorithms that work directly on TDOA-based locating systems' channel impulse responses. The authors have described the signal and data prepossessing in-depth and demonstrated the effectiveness of the method in a variety of real-world scenarios. While their method matches traditional signal processing methods under line-of-sight conditions, it beats earlier methods under significant multi-path propagation. The addition of a movement model to the DL-based solution should help it perform better. They also proposed a technique for distributing the Convolutional Neural Network (CNN) so that it can be used in Real-Time Locating System (RTLS) designs. They came to the conclusion that they

should reconsider how they currently estimate TOAs and that they could be evaluated using ML or DL methodologies as well. Furthermore, they did not explicitly address the transmitting orientation, despite the fact that this has an impact on the resulting Channel Impulse Response (CIR).

Table 3 shows the review of a comparison between several approaches to optimizing geolocation and target tracking.

**Table 3.** Comparison between several approaches of optimizing geolocation and target tracking.

| Approach | Advantages | Drawbacks |
|---|---|---|
| Taylor Series | Easy to find the spread of the solution; and easy detect-converge failure [101,102]. | Complex mathematically, compared to simple plotting of lines of position (LOP) [101,102]. |
| MLE | Less effect in-sample error and the maximum likelihood estimator can develop by a considerable variety of estimation situations [77,103]. | Complex mathematically, especially when confidence intervals for the parameters are wanted [103]. |
| LS | It may use instead of MLE in many non-linear statistical software packages [76,85]. | Need synchronization between all sensors, affected by NLOS errors, and more than two sensors are needed [76,85]. |
| WLS | Produces less error variance compared to the LS estimator [87]. | Difficult to achieve the exact weights, only estimated weights are taken into account and affected by NLOS errors [87]. |
| GA | It can provide new and potentially useful solutions for the decision-making stage [102,104]. | Any unsuitable choice will make it difficult for the genetic algorithm to converge, or it may generate meaningless results [105]. |

## 5. Approaches of Optimal State Estimation Utilizing Filtering

In the 1960s, the state estimation was primarily established, and their development evolved to considerable applications such as Kalman filtering and robust filtering [18,106]. It applies all practical fields, namely chemical engineering, aerospace engineering, and robotics. At a given moment, the state estimation is known as the complete reproduction of the internal condition of the system.

### 5.1. Kalman Filter (KF)

Kalman Filter (KF) is additionally known as linear quadratic estimation (LQE), which is named after Rudolf E. Kálmán in the first development of state estimation in the 1960s. It is an algorithm that uses a series of measurements that may be observed over time [30,107,108].

Kalman Filtering Algorithm

The Kalman filter (KF) uses feedback control to estimate the state of a target. It estimates the process state at a given time and then receives feedback in the form of measurement noise. As a result, the Kalman filter equations are divided into two categories: (i) time update equations (*Prediction*), and (ii) measurement update equations (*Correction*).

(i) *Prediction* : The time update equations are in charge of projecting the current state and error covariance estimates forward at a time in order to obtain a priori estimates for the next time stage.

(ii) *Correction* : The feedback—that is, integrating a new measurement into the a priori estimate to produce an improved a posteriori estimate—is handled by the measurement update equations. Time update equations are also known as predictor equations, while measurement update equations are known as corrector equations. Indeed,

as shown in Figure 19, the final estimation algorithm resembles a predictor-corrector algorithm for solving numerical problems [107].
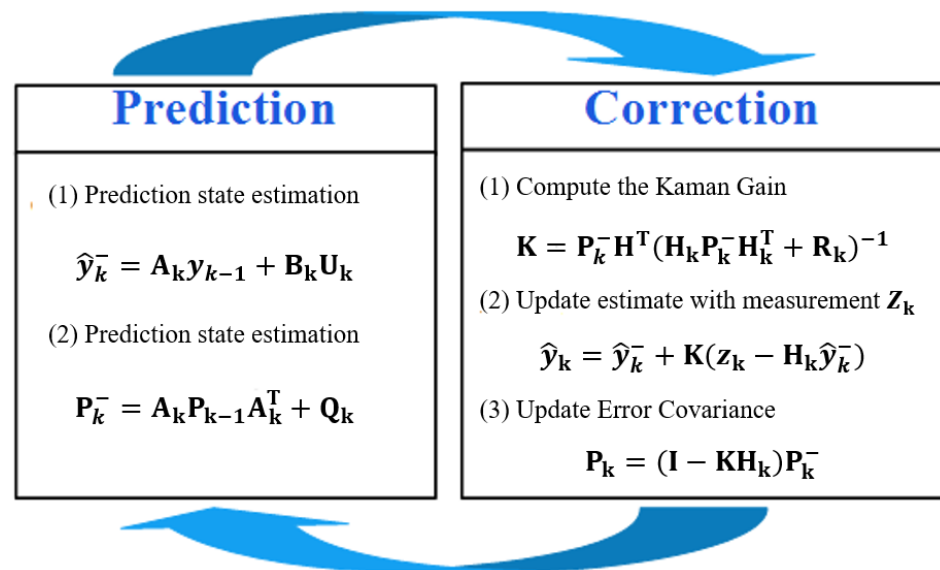
**Prediction**

(1) Prediction state estimation

$$\widehat{y_k^-} = \mathbf{A_k} y_{k-1} + \mathbf{B_k U_k}$$

(2) Prediction state estimation

$$\mathbf{P}_k^- = \mathbf{A_k P_{k-1} A_k^T} + \mathbf{Q_k}$$

**Correction**

(1) Compute the Kaman Gain

$$\mathbf{K} = \mathbf{P}_k^- \mathbf{H^T} (\mathbf{H_k P}_k^- \mathbf{H_k^T} + \mathbf{R_k})^{-1}$$

(2) Update estimate with measurement $\mathbf{Z_k}$

$$\widehat{\mathbf{y}}_k = \widehat{\mathbf{y}}_k^- + \mathbf{K}(\mathbf{z_k} - \mathbf{H_k} \widehat{\mathbf{y}}_k^-)$$

(3) Update Error Covariance

$$\mathbf{P_k} = (\mathbf{I} - \mathbf{KH_k}) \mathbf{P}_k^-$$

**Figure 19.** Kalman Filter prediction and correction algorithm.

### 5.2. Extended Kalman Filter (EKF)

Extended Kalman Filter (EKF) is an improvement of a conventional Kalman filter that has been widely used to solve non-linear estimation system problems. EKF works in higher-order terms, which include the Taylor expansions. It can approximate high non-linearity using first-order information. Many proposals have been given to improve the EKF. In addition, various applications have been used by EKF based on geolocation measurements. For example, Multilateration (MLAT) was used to overcome the problems caused by the drawbacks of Automatic Dependent Surveillance-Broadcast (ADS-B), which is considered one of the most important technologies in maneuvering and air traffic control [35]. The authors studied the problem of position precision and enhancing the robustness of the monitoring systems. Therefore, they proposed EKF based on hybrid TDOA/AOA measurements for the ADS-B/MLAT positioning system. Numerous experiments in various scenarios, such as TDOA individual or hybrid AOA/TDOA, were implemented. From the simulation results, one can observe the improvement of the geolocation accuracy and enhancement of the robustness of the surveillance systems [109].

Figure 20 illustrates the geometry distribution of static sensors and moving targets in the simulation. In the simulation scenario, four (04) stationary sensors distributed around a route were considered to receive signals from two spatially separated stations. Using time-delay and direction of arrival between transmitters (emitters) and receivers (sensors), three measurements of TDOA were obtained, as well as AOA, which was implemented as input parameters into EKF [109].
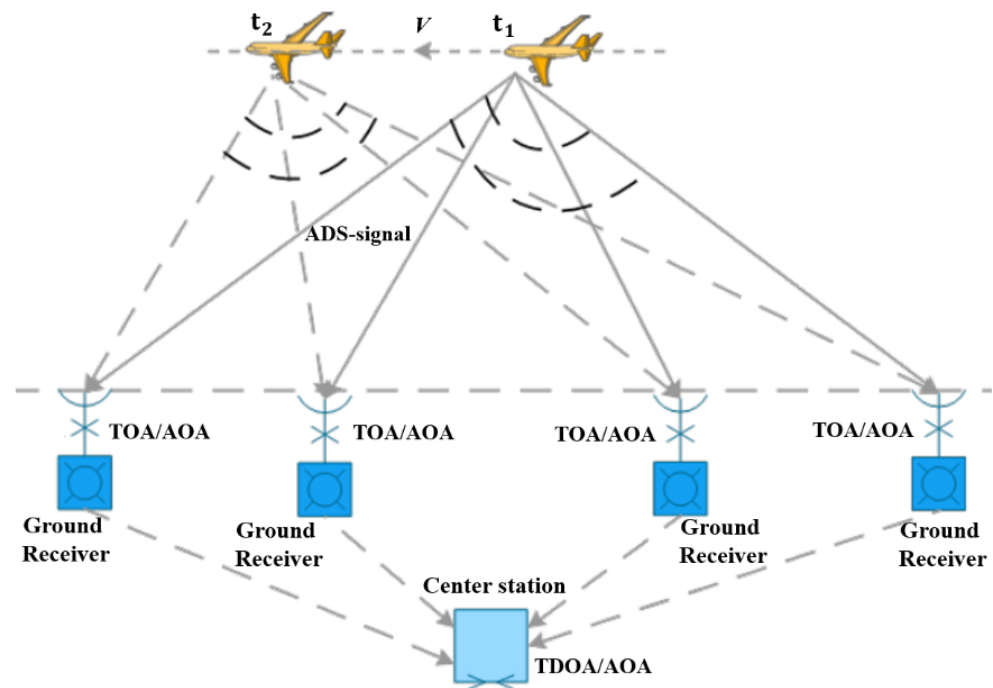
**Figure 20.** Geometry distribution of static sensors and moving targets in the simulation [109].

*5.3. Adaptive Extended Kalman Filter (AEKF)*

The adaptive extended Kalman filter is a viable technique for dealing with cases where there is little previous statistical information or where the estimation environment is evolving. Adaptive technology is used in a variety of areas, including adaptive control, in addition to filtering. Deep space probes can boost their navigation efficiency using two separate methods. The first is to create better error models that can represent the navigation system more realistically, and the second is to improve trajectory and sensor error estimation. Only the latter is taken into account in the current issue. To ensure effective navigation efficiency, an adaptive filter for measurement noise estimation is required. In an Inertial Navigation System/GPS (INS/GPS) integrated navigation system, adaptive Kalman filters are used to deal with the issue of unreliable measurement noise variance [110,111]. In [112], localization and mobile target tracking using TDOA/FDOA measurement with AEKF have been proposed. The framework of localization and target tracking, which have been considered, is exhibited in Figure 21a. In addition, Figure 21b exhibits the considered Simulink to achieve UAV tracking based on TDOA, FDOA and AOA proposed by authors.

The AEKF is suggested for updating the noise covariance at each estimation state. In this study, the simulation results show a trajectory of the mobile target on Earth. In order to demonstrate the tracking performance of the AEKF algorithm, 100 runs of Monte Carlo simulation results were achieved. The simulation results show considerable optimization for target tracking precision and the algorithm performance comparison with hybrid TDOA/FDOA and TDOA-only measurements. In addition, RMSE has recorded the reduction of about 32.53% and 39.09% in position and velocity, respectively, when employing TDOA/FDOA instead of TDOA individually [112].

From the Figure 22, we can note the performance improvement of target tracking estimation when we used the AEKM and ACKF compared to other filters.

(**a**)



(**b**)
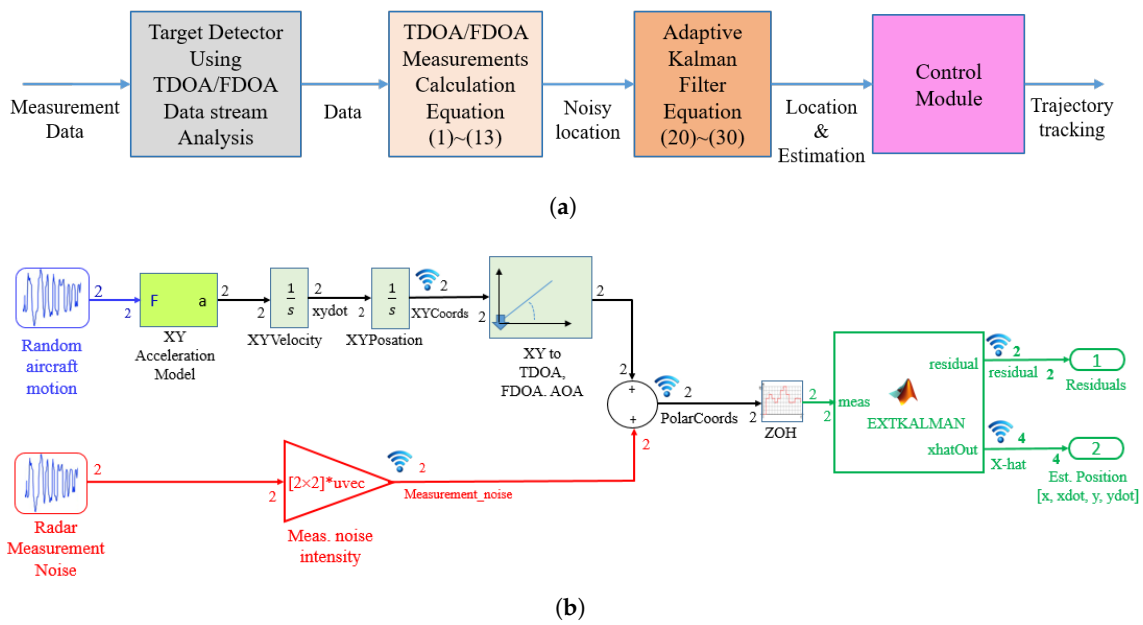
**Figure 21.** Structure and Simulink of algorithms for target tracking estimation (modified into Adaptive Extended Kalman Filter with TDAO/FDOA/AOA measurement). (**a**,**b**) show the framework of localization and target tracking using A EKF based on TDOA/FDOA measurements and Radar tracking using MatLab Function Block respectively. (**a**) [112], (**b**) [113].
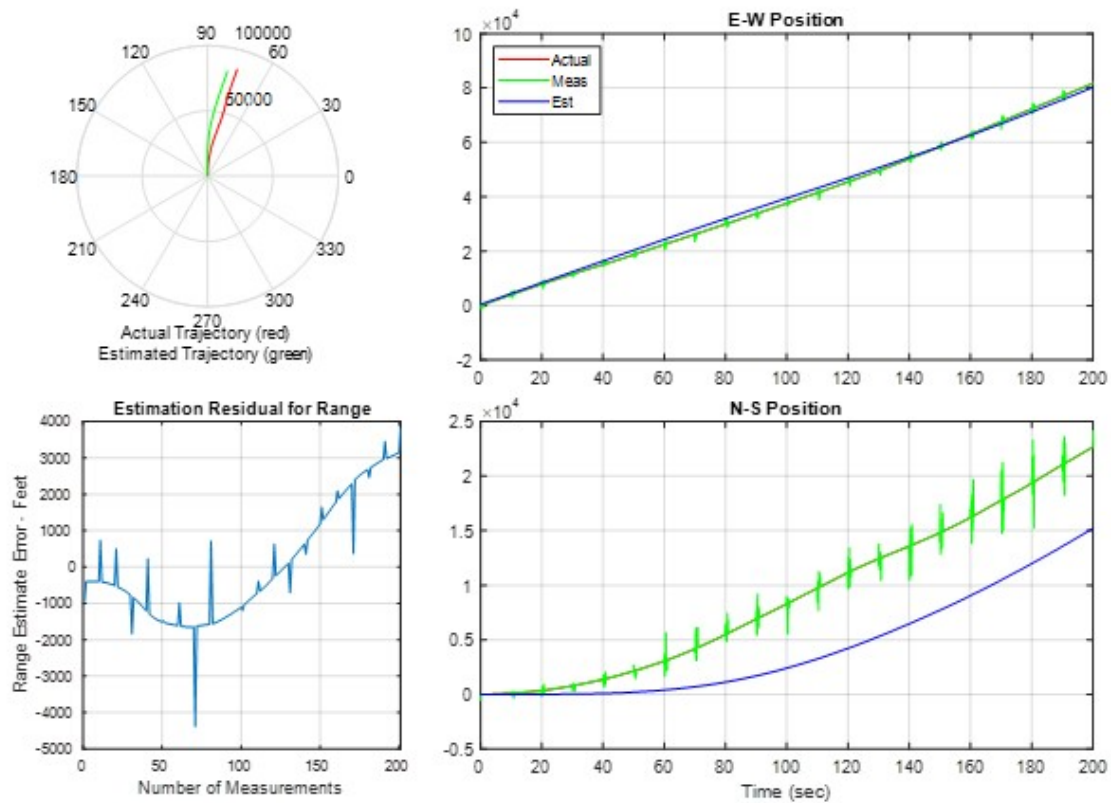


(**a**) EKF target tracking, trajectory diverges.

**Figure 22.** *Cont.*
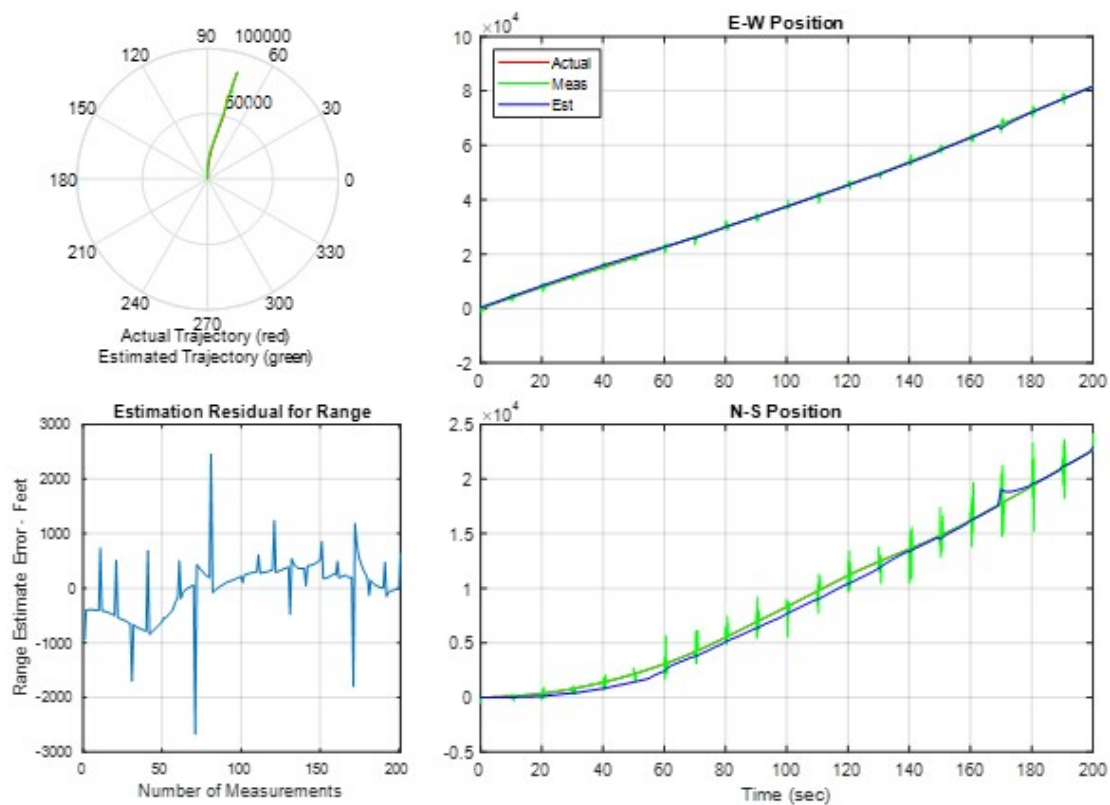
(**b**) Adaptive EKF target tracking estimation efficiency. Authors' own elaboration.

**Figure 22.** Performance comparison of considered filters for UAV tracking. Authors' own elaboration.

### 5.4. Cubature Kalman Filter (CKF)

Cubature Kalman Filter (CKF) is a spherical-radial cubature rule that makes it possible to numerically compute each moment of a new state, which is encountered in the non-linear Bayesian filter [114].

Arasaratnam et al. have derived an algorithm from a third-degree spherical-radial cubature rule, which provides a position of cubature points scaling linearly with the state-vector dimension. Because of that, the authors proposed a CKF that can provide a systematic solution for high-dimensional non-linear filtering problems. Experimentally, two non-linear state estimation problems were tested. In the first problem, to calculate the second-order statistics of a non-linearly transformed Gaussian random variable, the proposed cubature rule was employed. In the second problem, the CKF was utilized to track aircraft maneuvering. Eventually, they concluded that both experiments prove the enhanced performance of the CKF compared to conventional non-linear Kalman filters [115].

In [116], high degree non-linear CKF was considered to estimate the position and velocity of speedy UAV. From Figure 23, it can be noted that the proposed filter (CKF) achieved much better performance trajectory tracking compared with other Gaussian filters.

In 2009, Cao et al. considered the localization and target tracking problem using the Constrained Kalman Filter (CKF) based on measurements of TDOA and DOA. The study assumed that measurement noises are to be independent and identically distributed (i.i.d.). Moreover, minimum mean square error (MMSE) has been estimated by utilizing a pseudo measurement model that imposes a quadratic constraint on the state vector associated with the Ground Moving Target (GMT) dynamics. A solution to a similar quadratically constrained MMSE estimation problem was the first derivation by the authors. They recommended compensating for the hard constraint by its expectation in order to randomize the state vector for the GMT process. CKF was developed for those problems involving quadratic constraints and is appropriate for localization and tracking of GMTs and UAVs

based on TDOA and DOA measurements. In this scenario, two UAVs were considered as sensors to geolocate and track the Ground Moving Targets (GMT). CKF based on TDOA and DOA measurements was proposed to achieve high accuracy of target estimation and compare the performance with conventional KF. The simulation result of the proposed CKF appears better than the conventional KF [25].
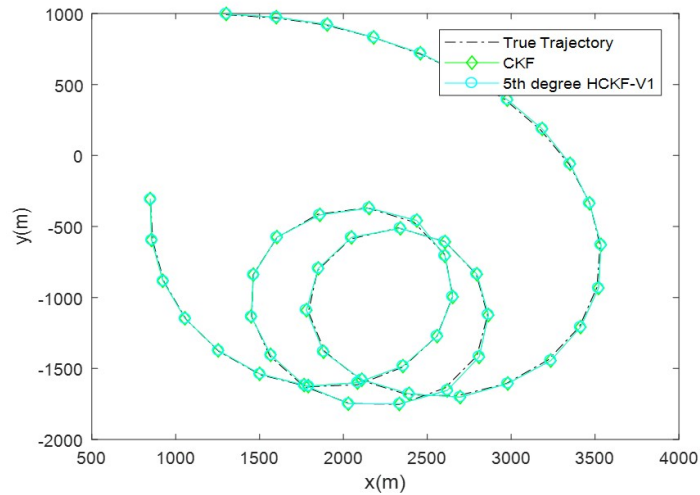


(**a**) UAV trajectory tracking using CKF and high degree CKF. Authors' own elaboration.
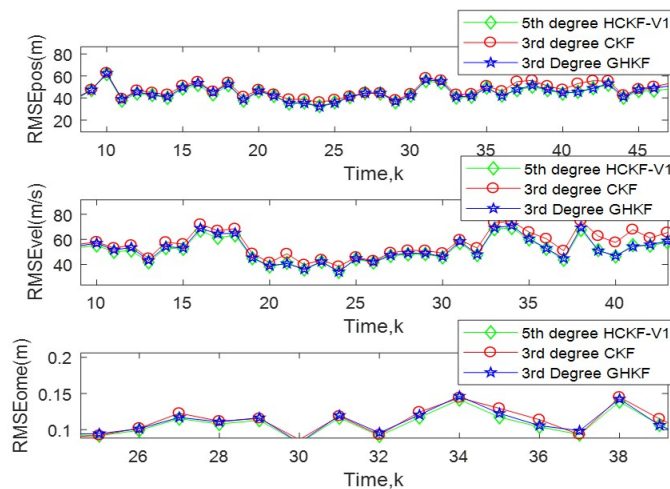


(**b**) RMSE performance of UAV estimation (position, velocity, and rotation). Authors' own elaboration.

**Figure 23.** Performance comparison of 5th degree CKF non-linear filter with EKF, UKF, and CDKF for UAV tracking [116].

### 5.5. Particle Filter (PF)

The particle filter (PF) is a technique for estimating the hidden states of non-linear and/or non-Gaussian systems and is very accurate. As a result, a particle filter-based track-before-detect approach is proposed, in which the particle posterior density distribution is directly estimated using beam-former output energy rather than bearing measurements, avoiding measurement-to-track interaction issues [117]. Regarding the estimation of movable systems from partial observations of internal states, particulary when random disturbances are present in the sensors [118], the gap in the filtering design was resolved. The discovery of the particle filters in 1996 by Del Moral paved the way for estimating the posterior distributions of the states of some Markov processes under noisy

and partial observations [119]. The geolocation measurement is one of the applications of particle filters.

Jeong et al. proposed a moving target tracking algorithm that used a particle filter based on TDOA/FDOA measurements by stationary sensors. Four base stations were considered to work as sensors that receive emitted signals from the dynamic target. From that signal, the time delay and frequency Doppler were measured, and TDOA/FDOA were calculated, which were used as input parameters to the PF algorithm.The authors established that PF operates with the non-linear properties of the moving target tracking problem successfully. In addition, they concluded that the performance of the proposed algorithm outperforms the one based on the EKF [120].

Figure 24 shows a performance comparison of EKF and PF for accurate target tracking estimation of the authors' own elaboration. From the figures, it is noted that the Pf algorithm is highly accurate for estimating the target compared to EKF.
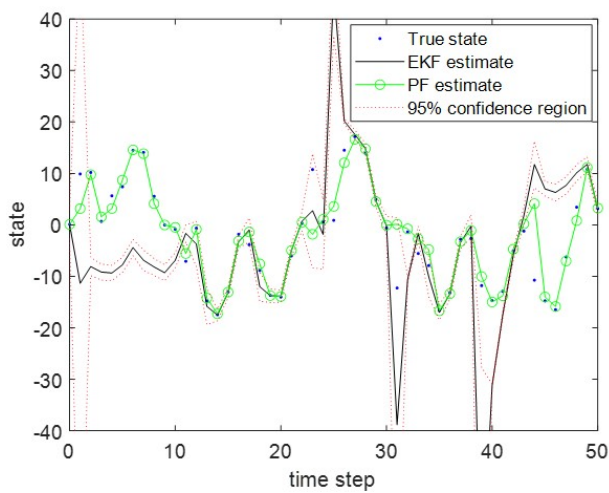


(**a**) Time series EKF versus PF with 300 particles.
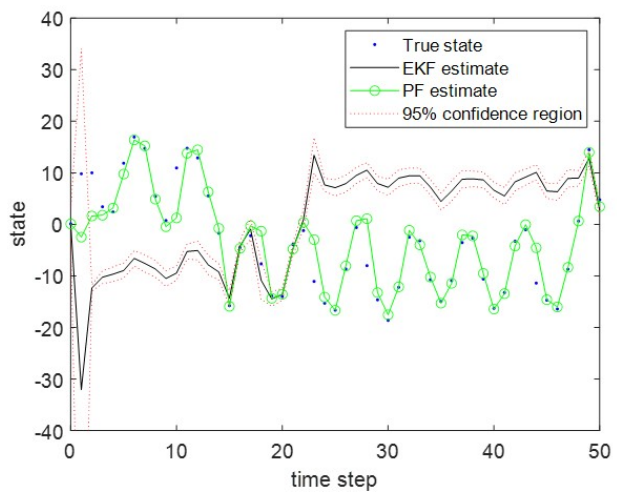


(**b**) Time series EKF versus PF with 1000 particles.
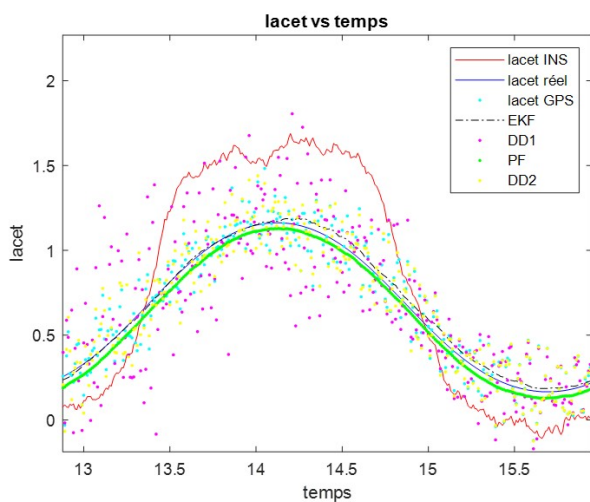


(**c**) AHRS-heading angle EKF versus PF with 500 particles.
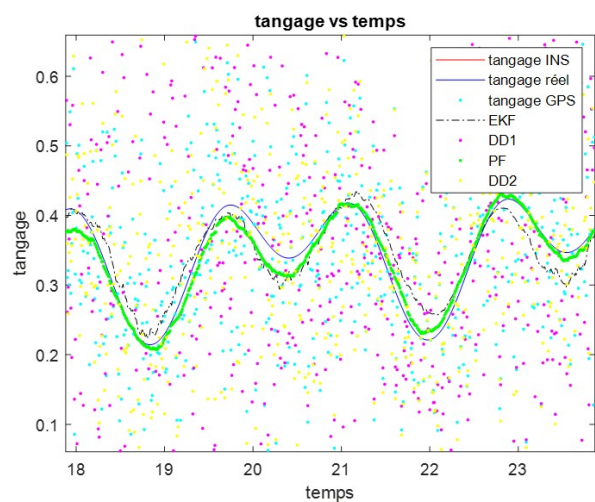


(**d**) AHRS-Pitchangle EKF versus PF with 500 particles.

**Figure 24.** Performance validation of EKF, interpolation filters based on divided differences called: DDF 1st Order, 2nd Order and Particle filter PF algorithms applied to AHRS attitude estimation. Heading and pitch angles are estimated in radians based on an INS/MultiGNSS antenna coupling approach. Authors' own elaboration.

### 5.6. Gaussian Mixture Model (GMM)

The Gaussian Mixture Model (GMM) could be a parametric likelihood probability density function that is represented as a weighted sum of Gaussian element densities. It is for the most part utilized as a parametric model of the likelihood distribution of persistent estimations such as sounding-tract, which related spectral features in a speaker acknowledgment framework [121].

We have also developed robust non-linear filters for navigation problems which we could extend easily to geolocation and target tracking problems. From Figure 25, it can be observed that both the speed and attitude estimation have improved by the derivation of GMM EKF, GMM-UKF, GMM-CKF and GMM-CDKF with CRLB and approximate CRLB bound from the authors' own elaboration.
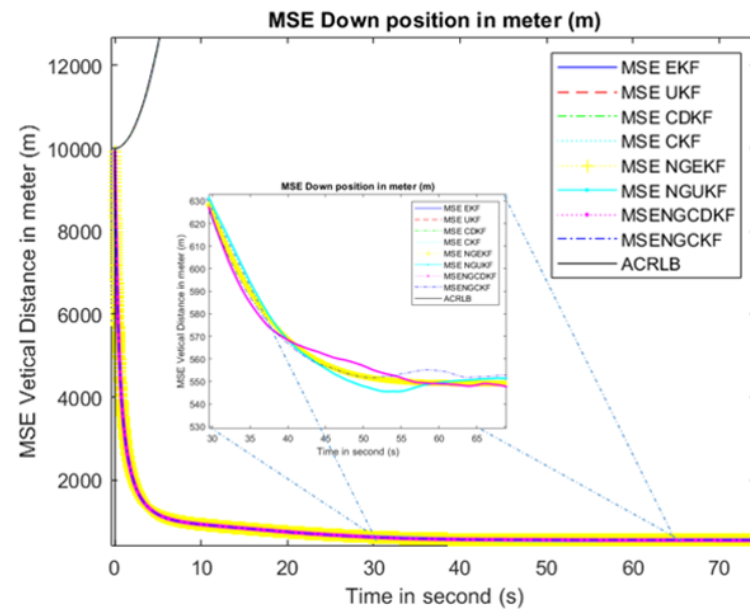


(**a**) RMSEs of position estimate under non-Gaussian measurement noises.
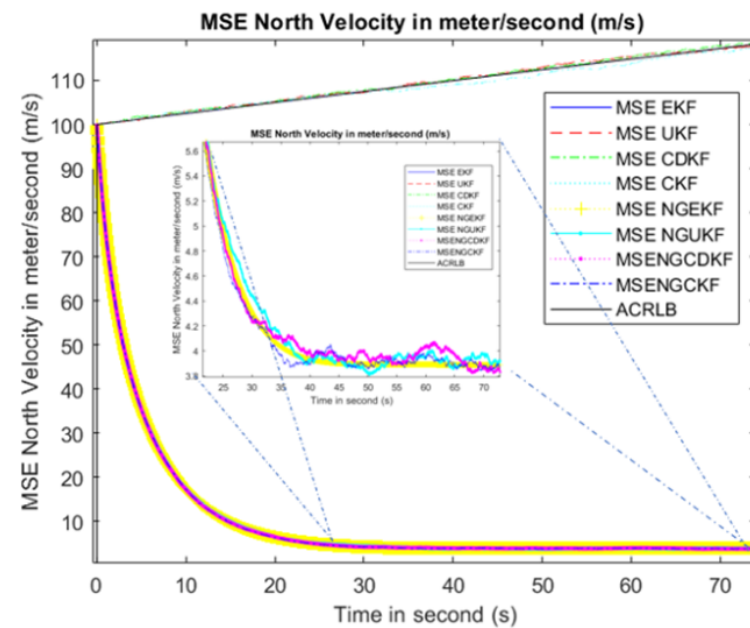


(**b**) RMSEs of velocity under non-Gaussian measurement noises.

**Figure 25.** Performance comparison of GMM non-linear filters for robust navigation and information fusion algorithms. Authors' own elaboration.

In [122], the comparison of three non-linear filters for estimating the position and velocity of a moving emitter and their result analysis was carried out collected by two UAVs flying over the area of monitoring using TDOA measurements. A multiple-model filter (MMF) with UKF Bank and an MMF with EKF Bank and a Gaussian mixture measurement integrated track splitting filter (GMM-ITSF) based Gaussian mixture (GM) model-based posterior PDF is utilized in the three proposed algorithms. The non-linear filters that are considered in the comparison are a multiple-model filter (MMF) with UKF Bank and an MMF with EKF Bank and a Gaussian mixture measurement integrated track splitting filter (GMM-ITSF). The performance of estimation errors was verified and analyzed using the derived CRLB. The performance analysis clarified that the UKFB had a better performance. Furthermore, MM-ITSF had a smaller number of diverged tracks.

### 5.7. Multiple Quadrature Information Filters (MQIFs)

Multiple Quadrature Information Filters (MQIFs) is a developed algorithm package of a recursion, non-linear Kalman filtering. The means and covariance of all conditional densities using the Gauss–Hermite quadrature rule in different degrees can be computed using this package [23,123].

In [124], the authors focused on the algorithm of Quadrature Kalman filter (QKF), which was recently developed. It is mentioned that with a Gaussian assumption and based on Gauss–Hermite quadrature rules, the QKF can tackle arbitrary non-linearities. The complexity reduction technique for the QKF based on the partitioning of the state-space, referred to as the Multiple QKF, was studied. The dimensionality reduction has been reduced with the aid of partitioning schemes.

Figures 26 and 27 illustrate the performance validation of the non-linear filter considered, as well as the scenario and Geometric Dilution of Precision (GDOP) of the LEO satellite.



(**a**) The case of the estimated covariance matrix equals the real covariance matrix

(**b**) The case of the estimated covariance matrix equals fifty times the real covariance matrix.
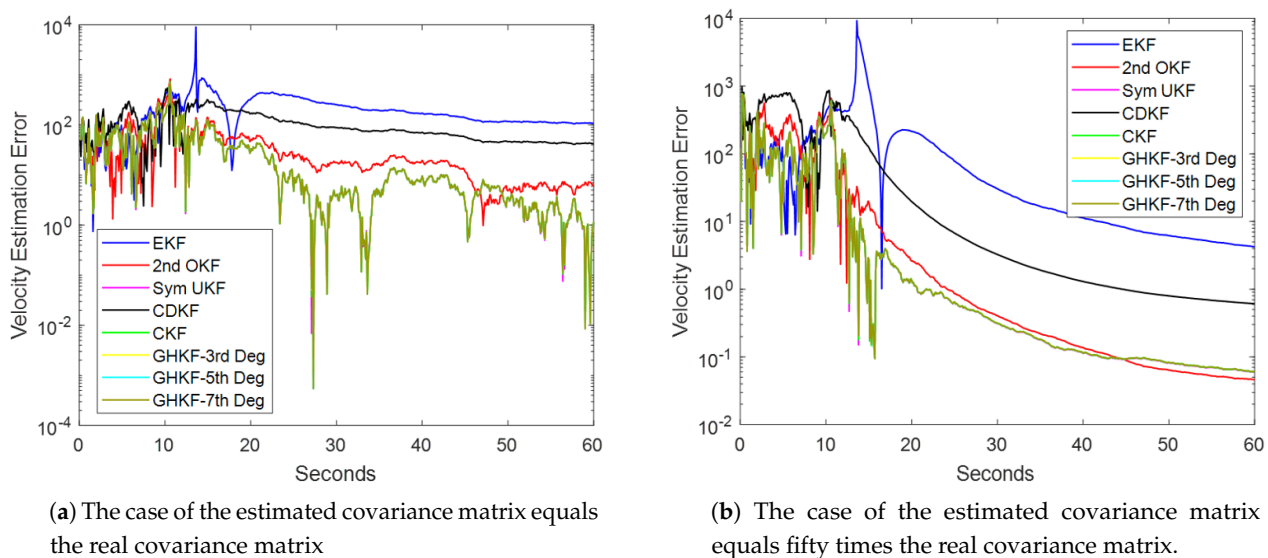
**Figure 26.** Performance validation of EKF, 2nd Order KF, UKF, CDKF, CKF with GHKFs algorithm. This study focused on a complexity reduction technique for the Bayesian filtering based on the partitioning of the state-space. It proved that the partitioning schemes can efficiently be used to overcome the curse of dimensionality in the GHKF. The simulation result shows that a nearly-optimal performance can be attained using GHKF with non-linear filtering problems. Authors' own elaboration.
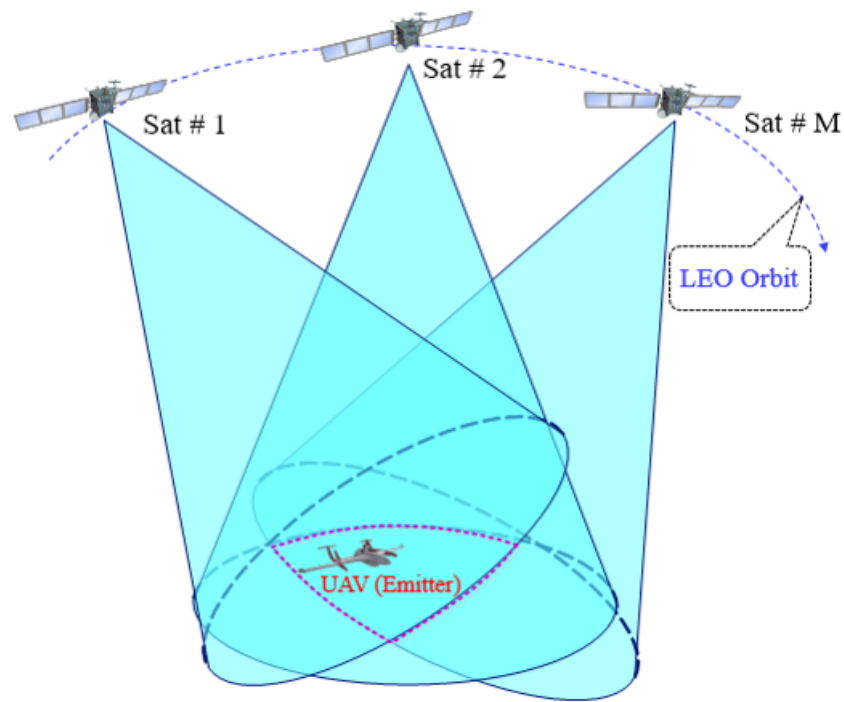
(**a**) Geometry of multi-sensors (LEO satellite).
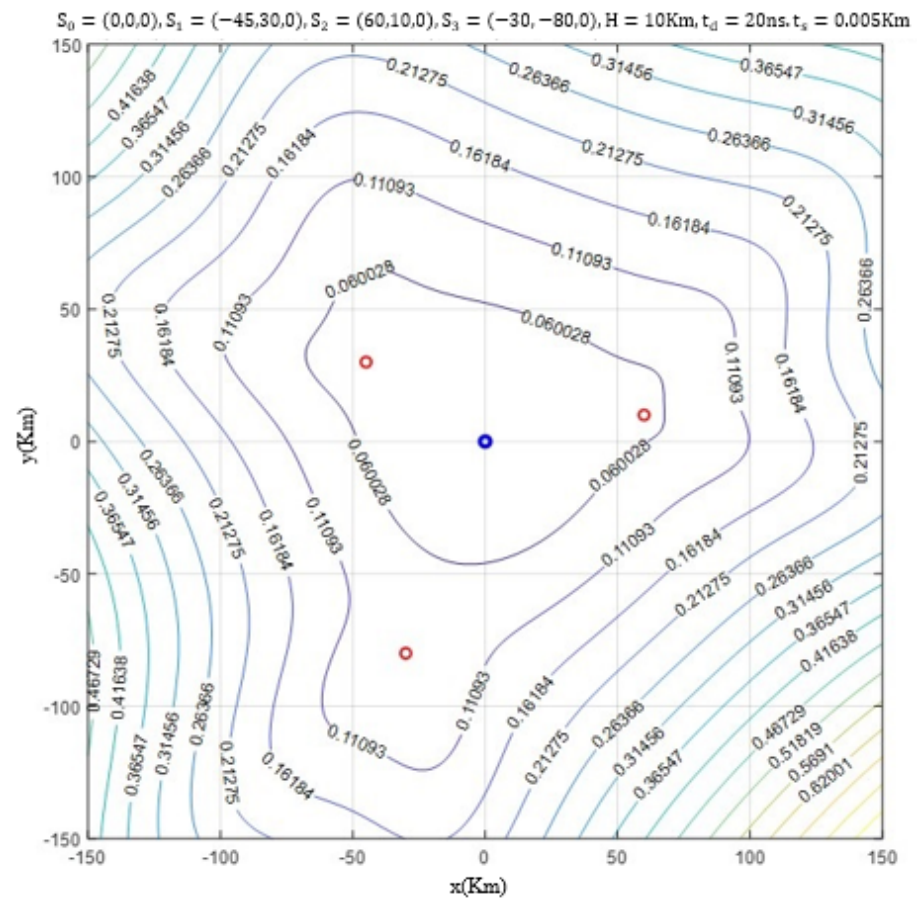


(**b**) TDOA based GDOP for instantaneous sensors distribution.

**Figure 27.** The geometry of multi-sensors (LEO satellite) and GDOP of the sensors for achieving the most precise estimation of a moving target (UAV) proposed in the simulation scenario. Authors' own elaboration.

Scenario Simulation of RFI UAV Flying in the North Latitudes

Numerous scenarios of geolocation and target tracking using considered filters based on TDOA, FDOA, TDOA/FDOA, and PDOA/FDOA measurements have been implemented. Multi LEO satellites were considered for geolocation and UAV tracking in these scenarios. Figure 28 shows a UAV embedded with RFI sources is flying under LEO satellite's visibility and sensitivity, which is subject to a problem statement of UAV target tracking by multiple satellites. Below, some simulation results are shown using high-degree non-linear filtering.

In the simulation scenario, three (03) LEO satellites were considered as sensors to estimate UAV tracking flying above Canada. The initial point was selected from the reference station on the roof of ETS-Montréal. The simulation results are based on 100 Monte Carlo runs. The initial estimate $x_0$ values with different uncertainty level values were introduced gradually. They are given as follows: $x_0 = [0\,\text{m}, 0\,\text{m/s}, 0\,\text{m}, 0, 0\text{deg/s}]^T$ and $P_0$ being the initial covariance: $P_0 = \text{diag}(100\,\text{m}^2, 10\,\text{m}^2/\text{s}^2, 100\,\text{m}^2, 10\,\text{m}^2/\text{s}^2, 100\,\text{m}\,\text{rad}^2/\text{s}^2)$. The metrics used to compare the performance of various filters was the average root mean square error (ARMSE).

From Figures 29–33, it can be observed that the algorithm performance based on hybrid TDOA/FDOA measurements is the best compared to TDOA, FDOA, and TDOA/PDOA measurements.
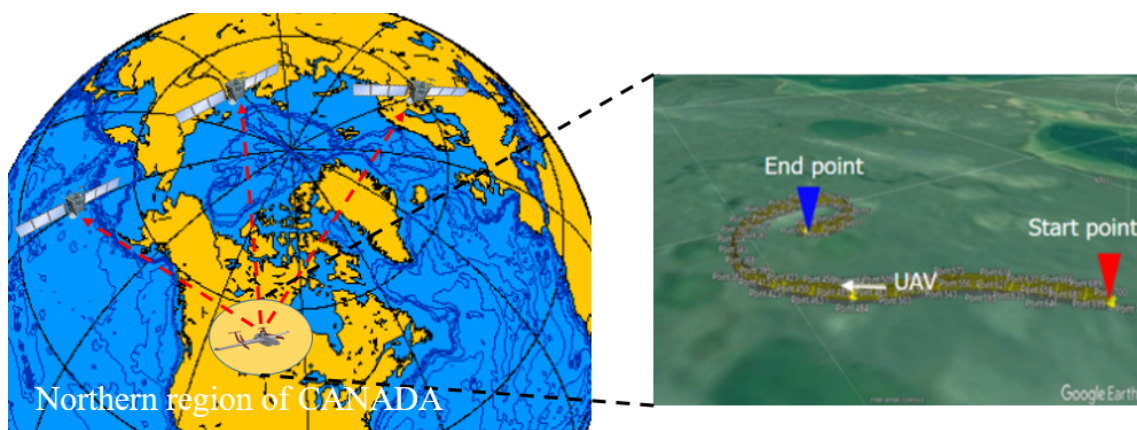


**Figure 28.** UAV target tracking in the northern region of Canada.



(**a**) Trajectory of sensors and target.

(**b**) Tracking of the proposed filter.
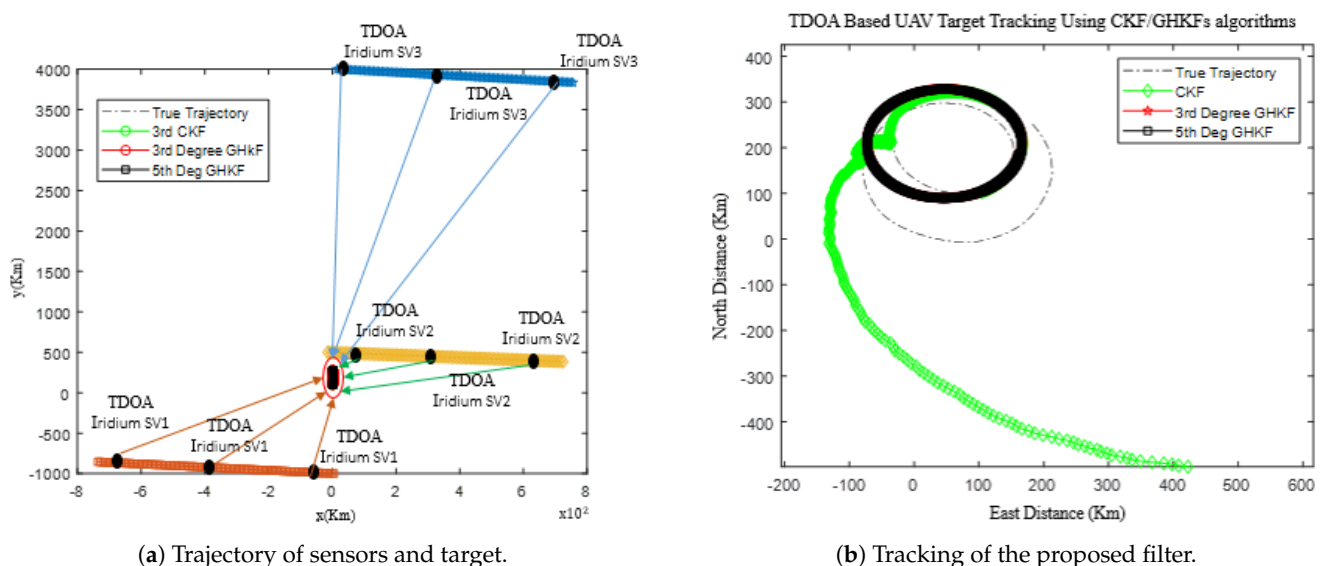
**Figure 29.** Three (03) Iridium satellites were employed to track a UAV based on a TDOA measurement. Authors' own elaboration.
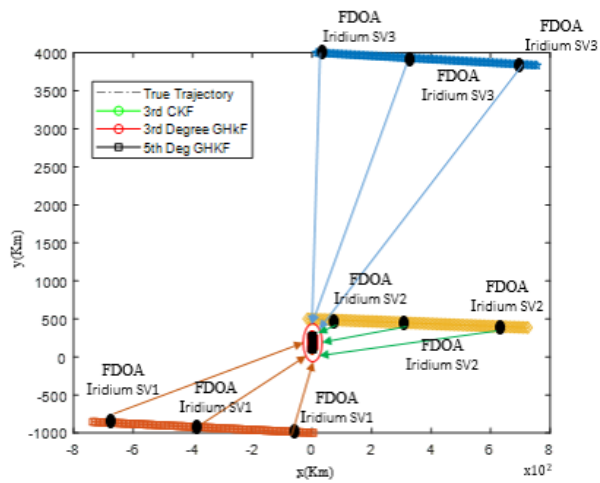
(**a**) Trajectory of sensors and target.
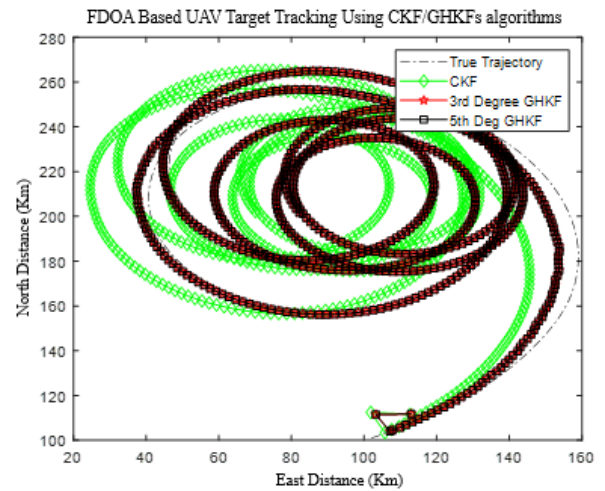


(**b**) Tracking of Proposed filter.

**Figure 30.** Three (03) Iridium satellites were employed to track a UAV based on an FDOA measurement. Authors' own elaboration.
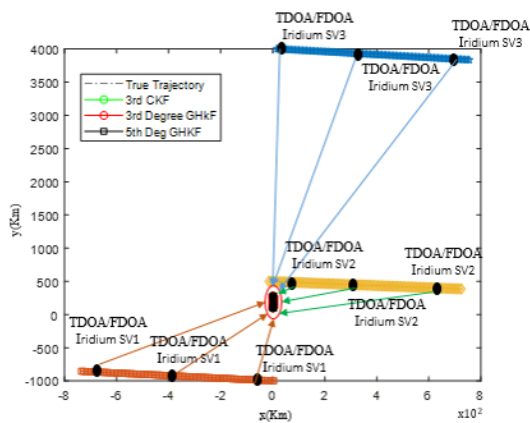


(**a**) Trajectory of sensors and target.
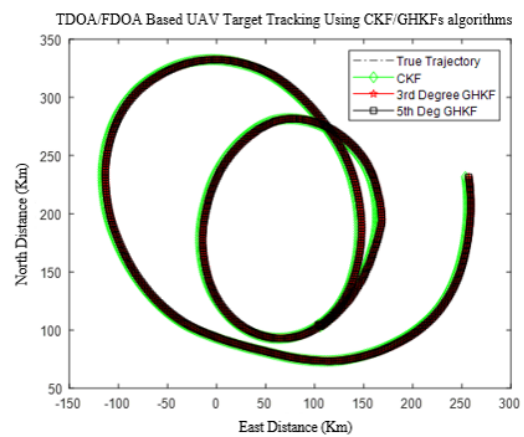


(**b**) Tracking of Proposed filter.

**Figure 31.** Three (03) Iridium satellites were employed to track a UAV based on a TDOA/FDOA measurement. Authors' own elaboration.
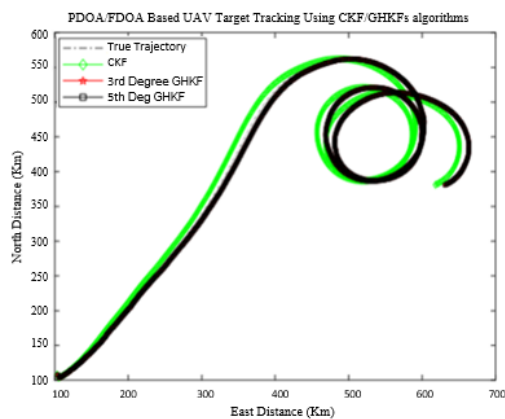


(**a**) UAV tracking.
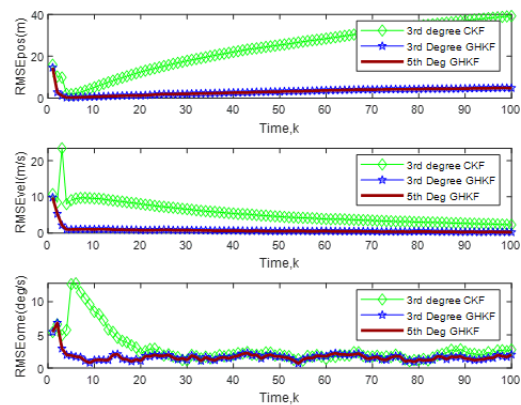


(**b**) RMSE of algorithm performance.

**Figure 32.** Target tracking and RMSE for verifying the algorithm performance. In the first simulation scenario, three (03) Iridium satellites were considered as sensors to estimate the trajectory and velocity of the UAV based on hybrid TDOA/PDOA measurements. Authors' own elaboration.
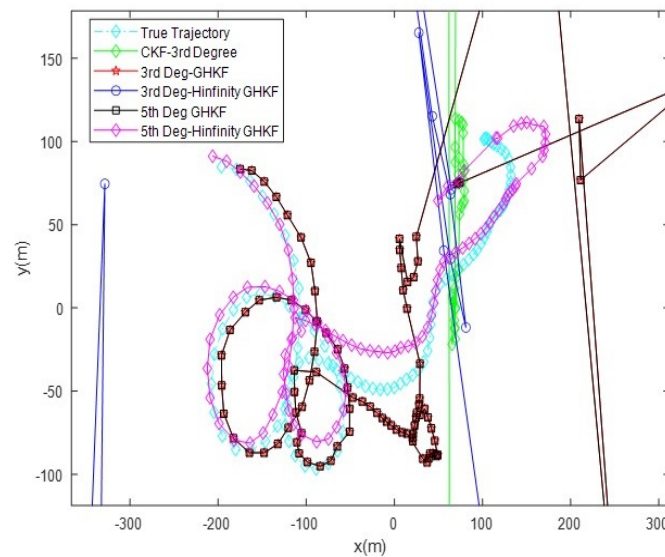
(**a**) Maneuvering UAV tracking estimation using CKF 3rd, GHKF 3rd, $H_\infty$/GHKF 3rd, GHKF 5th , and $H_\infty$/GHKF 5th, true trajectory.
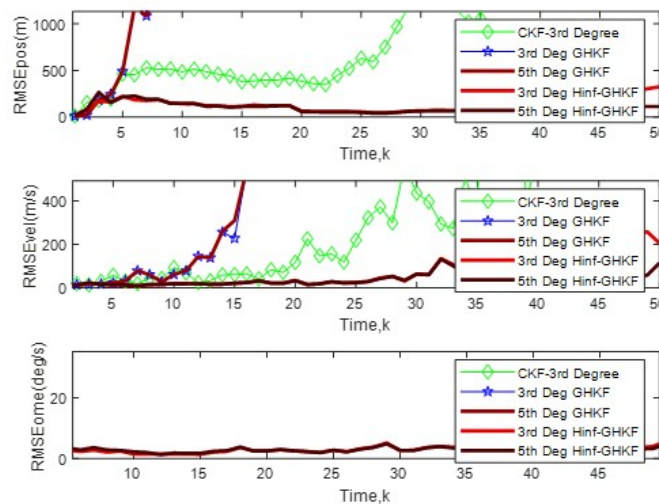


(**b**) RMSE based on TDOA/FDOA: Performance results of $H_\infty$/GHKF 5th and $H_\infty$/GHKF 3rd compared to CKF 3rd, GHKF 3rd, and GHKF 5th

**Figure 33.** Comparing the performance of target tracking algorithms [21].

### 5.8. $H_\infty$ Filter

$H_\infty$ is a developed filter employed to overcome the degradation that affects the Kalman Filter performances and results in unreliable state estimates. The first discovery of $H_\infty$ was in the 1980s, and it is a new development compared to Kaman Filter. Therefore, there is a wider area for extra work and development in $H_\infty$ filtering than Kalman filtering [30]. The authors of [125] proposed a decentralized $H_\infty$ /UKF that enhances the strength of the $H_\infty$ standards developed in robust control to address a non-Gaussian process and measurement noise as well as unreliable state estimates. To address the strong model non-linearities, the advent of UKF has been utilized by the proposed algorithm under uncertainties. The linear-like batch-mode regression model for statistical linearization approach equivalent to the linear Kalman filter is derived. The simulation result illustrates an RMSE comparison of the proposed algorithm performance with decentralized UKF with a measured terminal

voltage phasor (DUKFV) and a decentralized UKF with a measured terminal current phasor (DUKFI) in the presence of a non-Gaussian process and measurement noise.

In addition, it provided that the proposed $H_\infty$/UKF is capable of bounding the influences of numerous types of measurement and model uncertainties while achieving precise state estimates. Based on TDOA and FDOA measurements, the study focused on comparing the performance of non-linear filters for estimation of the location and velocity of a moving emitter. From Reference [125], the comparison shows that $H_\infty$/UKF is better than other conventional filters.

In 2011, Wang et al. proposed a novel algorithm that combines the $H_\infty$ filter into the particle filter (PF). The main purpose of combining $H_\infty$ with PF is a new particle sample of PF that will be taken by the $H_\infty$F algorithm [126]. Consequently, $H_\infty$F can take into account full current measurements. Moreover, the $H_\infty$F algorithm can adjust the gain inequality factor by adjusting the disturbance attenuation factor and achieve satisfying accuracy and robustness. The experimental results illustrate the estimated trajectory of the target by PF, KPF, and $H_\infty$/PF and present a comparison of an error estimated for a localization and target tracking using a PF, Kalman Particle Filter (KPF), and $H_\infty$/PF. The simulation and experimental results concluded that the proposed $H_\infty$/PF performed better than PF and the PKF in tracking maneuvering targets.

In Figures 34 and 35, it is interesting to observe how estimation accuracy was improved using $H_\infty$ mixed with Gauss Hermite Quadrature Kalman filters in regards to the geolocation and target tracking based on TDOA/FDOA measurements derived and implemented by the authors [21].



(**a**) Position RMSE under high uncertainty. Results of $H_\infty$/GHKF 5th and $H_\infty$/GHKF 3rd compared to CKF 3rd, GHKF 3rd, and GHKF 5th
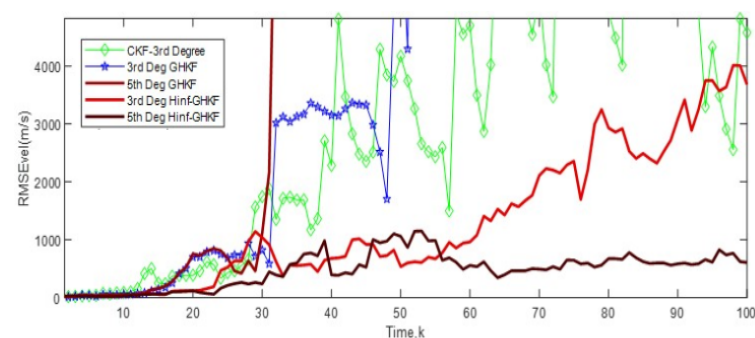


(**b**) Velocity RMSE under high uncertainty. Results of $H_\infty$/GHKF 5th and $H_\infty$/GHKF 3rd compared to CKF 3rd, GHKF 3rd, and GHKF 5th

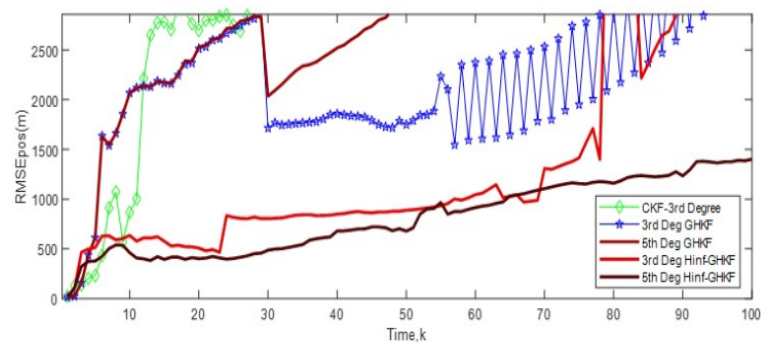**Figure 34.** Comparing the performance of target tracking algorithms. This study focused on comparing the performance of non-linear filters for estimating the location and velocity of a moving emitter based on TDOA and FDOA measurements. The comparison shows that the $H_\infty$/GHKF is better than other conventional filters [21].

**Figure 35.** GNSS signals data collection in a Montreal urban environment with high buildings as obstacles.

Table 4 displays a comparison between different filters employed in the optimal state estimation for an emitter source.

**Table 4.** Comparison between various filters used for optimal state estimation of target tracking.

| Filter | Advantages | Drawbacks |
|---|---|---|
| KF | Simple mathematially, and fast version [127]. | Working only in linear systems [127]. |
| EKF/UKF | Less complexity in the mathematical process, and easy to implement [128]. | A high initial estimation is required [128]. |
| AEKF | It can reduce the problem of non-linearity that face EKF [112]. | If the target has high rotational speed, the non-linearity error may increase [112]. |
| UKF | No need for the system to be linear [127]. | Mathematically costly, and more parameters need to tune [127]. |
| CKF | It is a better performance compared to UKF; it improves the state estimation vector [127]. | Limited use, just used at specific applications [127]. |
| PF | Flexible with multi-robot, more robust for unknown data-association issues [129]. | It depends on the number of particles employed. When updating equation iteration, it may produce a significant weight of particles [129]. |
| GMM | No need for too many parameters for learning, and it can achieve the best estimation utilizing the Expectation-Maximization (EM) Algorithm to maximize the log-likelihood [130]. | The achieved result of segmentation by GMM is not robust to noise measurement [130,131]. |
| MQIFs | The MQIFs deal with the highly non-linear nature of the mobile target-tracking problem successfully [23]. | The number of Gaussian phases increases exponentially over time [132]. |
| $H_\infty$F | It is capable of handling significant system uncertainties, overcoming outliers while obtaining an excellent statistical efficiency under Gaussian and non-Gaussian processes; observation noises, especially when it is combined with any Kalman filter [22]. | Complex mathematically [30]. |

In Table 5, geolocation and target tracking approaches, as well as algorithm specifications employed in the state-of-the-art methods, have been summarized. Consequently, we can note that the increasing number of sensors as well as combining more than one geolocation technique leads to an increase in the accuracy of the geolocation measurement. In addition, the scenarios of geolocation and emitter tracking that were verified in near-field environments were more precise compared to the scenarios in far-field environments. The distances between emitters and sensors are in the order of kilometres for far-field, while the distances will be shorter in near-field environments, which leads to fewer errors.

Employing hybrid filters such as GHKF/$H_\infty$, UKF/$H_\infty$, and EKF/$H_\infty$ may achieve high accuracy target tracking and estimation compared to using the individual filter.

*5.9. Real Data Collection from GNSS Receivers and Sensors Fusion*

GNSS constellation presently composed of GPS, GLONASS, Galileo, BEIDOU and SBAS augmentation satellites such as WAAS (USA), EGNOS (Europe), SDMC (Russia), GAGAN (India) are widely integrated and used in major navigation applications. Table 6 presents the current Space Vehicles (SV) employed in GNSS. Furthermore, many recent works were dedicated to counter the vulnerability of these constellations and their positioning accuracy, which can be degraded in harsh or denied GNSS environments. To achieve better performances, and based on several recent surveys, different data fusion, sensors fusion and information fusion with modified filtering algorithms were developed and proposed in the literature. Even with hundreds of satellite channels and multi frequency tracking capabilities with dual code/phase positioning methods, GNSS receivers may suffer from spoofing, jamming and interference, NLOS and multipath problems, and therefore need to be coupled with alternative higher-data-rate navigation sensors. In this survey, however, the benchmark and analysis were given to geolocate and target tracking algorithms and systems independently of GNSS receivers. The best alternative innovative solution is the use of LEO satellite signals of opportunity for localization and tracking. Presently, for the reasons mentioned above, they represent the best alternative Positioning, Navigation, and Timing (PNT) solutions.

**Table 5.** Summary of geolocation and target tracking algorithm specifications employed in the state-of-the-art methods.

| Ref. | Algorithm Employed | Accuracy | Geolocation Technique Used | Field Source | Sensor Type | No. of Sensors Used | Sensors State | Emitter Type | Emitter State |
|------|--------------------|----------|----------------------------|--------------|-------------|---------------------|---------------|--------------|---------------|
| [133] | GA | 30.9% | TDOA | near-field | active | 5 | stationary | active | stationary |
| [95] | GA | >60 m | TDOA | far-field | – | 3 to 5 | stationary | – | stationary |
| [134] | WLS-RW | higher precision | AOA, PDOA | near-field | passive | 1 + 2 reflectors | stationary | passive | stationary |
| [75] | WLA | high accuracy | TDOA, FDOA, d.D.rate | near-field | passive | 5 | moving | passive | moving |
| [135] | MoMo | 50 m | TOA, AOA | near, far | passive | 2 | moving, stationary | passive | moving, stationary |
| [136] | CFSSLS CFFSLS | 4.41 3.90 | TDOA | near-field | active | 7 | stationary | passive | stationary |
| [137] | MLE | demonstrate potential gains | CAF | near-field | – | 2 | moving, stationary | – | stationary |
| [138] | CWLS | good performance | TDOA | near, far | passive | 8 | stationary | passive | stationary |
| [139] | MLE | improve | RSS | near-field | active | 4 to 9 | stationary | active | stationary |
| [16] | Taylor Series | better accuracy | TDOA, FDOA | far-field | passive | 6 | stationary | passive | moving |
| [140] | ICWLS | good performance | TDOA, GROA | near, far | active | 8 | stationary | active | stationary |
| [141] | WLS | 25 m | TDOA, FDOA | near, far | passive | 5 | moving | passive | moving |
| [142] | WLS | high accuracy | TDOA, FDOA | far-field | passive | 10 | moving | passive | moving |
| [143] | UKF | high accuracy | TDOA, FDOA | far-field | passive | 2 | moving | passive | moving |
| [112] | AEKF | 32.53%, 39.09% | TDOA, FDOA | far-field | passive | multi-sensor | moving | passive | moving |
| [144] | PDA+ EKF/UKF | PDA better than NN | AOA | far-field | passive | 2 | stationary | passive | moving |
| [110] | AEKF | 0.15 km | TDOA, FDOA | far-field | passive | 4 | moving | passive | moving |
| [145] | MLE+ GMF | 500 m | TDOA/ AOA, TDOA/ FDOA | far-field | passive | 2 | moving | passive | moving |
| [25] | CKF | 200 m | TDOA/ DOA | far-field | passive | 2 | moving | passive | moving |
| [146] | GMM- CQKF | superior performance | TDOA, FDOA | far-field | passive | 2 | moving | passive | moving |
| [21] | GHKF/ $H_\infty$ | 50% | TDOA/ FDOA | far-field | passive | 3 | moving | – | moving |
| [147] | EKF, UKF,$H_\infty$ | high accuracy | TDOA | near-field | – | 4 | stationary | – | stationary |
| [148] | UKF, $H_\infty$ | 5.81% | – | far-field | passive | multi-sensor | moving | passive | moving |

**Table 6.** Basic information on GSSN constellations, Space Vehicle (SV) number, altitude platform, period of movement, frequency used, and most principles of the navigation system.

| | No. of SV (2015) | Orbital Plane | Inclination (Degree) | Altitude (Km) | Period | Frequencies (Civil Use) (MHz) | Coordinate Frame | Time System | Coding |
|---|---|---|---|---|---|---|---|---|---|
| GPA (USA) | 28 | 6 | 55 | 20,200 | 11 h 56 min | L1:1575.42 L2:1227.60 L5:1176.45 | WGS-84 | GPST | CDMA |
| Galileo (Europe) | 30 | 3 | 56 | 19,100 | 11 h 15 min | E1:1575.4242 E5b:1207.14 E5a:1176.45 | GTRF | GST | CDMA |
| GLONASS (Russia) | 26 | 3 | 64.9 | 23230 | 11 h 15 min | 1106 ∼ 1616 1246 ∼ 1257 | PZ-90 | UTC (SU) | FDMA |
| BEIDOU (China) | 27 (+5 GEO +3 IGSO) | 3 | 55 | 21,528 | 12 h 53 min 24 s | B1:1575,42 B2:1191,79 B3:1268,52 | CGCS2000 | BDT | CDMA |

In Figure 35, one can observe different GNSS outlier situations collected during real tests in Montreal, downtown between high buildings. Data were collected and processed a posteriori for INS/GNSS coupled approaches subject to other results and works such as in [149–154]. Different effects could be identified in such situations with alternative solutions mitigating multi-paths, NLOS biases, GNSS satellite visibility masks due to buildings, measurement interruption, and interference, etc.

*5.10. Real Data Collection from LEO Satellites*

In the majority of cases, software-defined radios (SDR) with passive antennas in receiver modes are used on-board vehicles and aircrafts (UAV) to collect raw data from different LEO satellites, such as Iridium Next, Orbcomm, Globalstar and in the future, OneWeb, Starlinks, etc. [94,155–157]. The goal is to identify the signal of interest (Tones) with channel frequency and develop or design an adapted receiver to track the frequency, phase and extract Doppler shift-Doppler rate for positioning and localization. In the following, in Figure 36, one can observe the electronic bench installation on-board the aircraft with LEO L-band (1626.27–1626.43 MHz) and VHF/UHF antennas (400.1 MHz) for Iridium Next and Orbcomm data collections, respectively [94]. The optimal sampling rate can be obtained by maximizing the SNR optimization function. That means, at the moment, for each system, a new design and parameter identification for tone detection and tracking are necessary [94].

In Figure 36, one can observe that a differential positioning and localization mode is possible to achieve in addition to the absolute mode by using LEO satellite signals of opportunity. The huge potential of the present and future constellations, such as described in Table 7, demonstrate the feasibility and the reliability of these constellations when the localization and target tracking would be considered in a denied GNSS environment [94]. Until now, no open public dataset regarding LEO SoOP-based positioning systems has been released; meanwhile, considerable efforts and original results were achieved by the authors of [94,155–157].
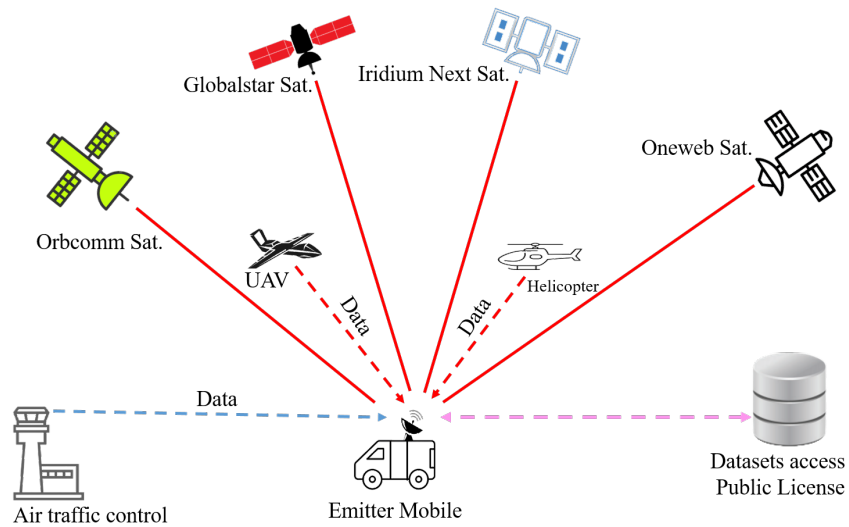
**Figure 36.** Geometry of sensor and target location in 3D using absolute and differential SOP processing from multiple LEO constellations.

**Table 7.** Basic information on satellite formation, satellite constellations, principles, satellite altitude, frequency bands, and most popular LEO sat. status of the satellite.

| Satellite Constellations | Altitude of Orbit (Km) | Number of Satellites | Frequency Band | Status (2021) |
|---|---|---|---|---|
| SpaceX-Starlinks | 350–550–1150 | 12 + 30,000 (Upcoming) | Ku, Ka, and V | 1735 in Orbit |
| Orbcomm | 650 | 50–52 | VHF | Completed |
| Globalstar | 1414 | 48 | L, S, and C | Completed |
| Iridium Next | 780 | 66 | La and Ka | Completed |
| Oneweb | 1220 | 648 | Ku and Ka | 218 in Orbit |
| Boeing | - | 2956 | V and C | Not yet launched |
| Samsung | - | 4600 | V | Not yet launched |

## 6. Conclusions

The most conventional and recent techniques of geolocation and target tracking have been reviewed in this paper. Furthermore, different geolocation algorithms (such TS, MLE, WLS, KF, EKF, AEKF, UKF, GHQF, $H_\infty$, GA, DL, etc.) demonstrated various levels of performances depending on the localization environment and sensors network architecture. Different scenarios and cases could be classified and carried out; static beacons (sensors) with stationary RFI detection and localization, static beacons with mobile RFI detection and localization, as well as mobile sensor networks with mobile RFI detection and localization or detection and tracking. Each of the techniques and methods mentioned from basic least square to recursive LS and other variants, in addition to Kalman filter and more sophisticated versions, such as UKF and GHKF, the dynamics of the RFI and non-linearity degrees of the state estimation problem have a direct impact on the algorithm selection and implementation. Each method has its own advantages and drawbacks. Important factors of real-time processing or digital processing present constraints that engineers in this field must adapt to using the most optimized techniques, e.g., the introduction of different optimization techniques, machine learning and artificial intelligence (AI).

Depending on the initial conditions, assumptions and scenario limits and constraints, the same technique or method could perform well or poorly, as explained. Especially when selecting the best measurement model and data to be processed, discussions about

TDOA, FDOA, AOA, PDOA and multiple combinations of these techniques are possible solutions depending on the sensors network key parameters, nodes, beacons, number of nodes, static, mobile beacons, distance between RFI source and beacons, and nodes, etc. Therefore, in order to develop realistic algorithms with real-time and real environment capabilities and efficiency, uncertainty of the environment, randomised changes, and time varying noises modelling have to be considered in order to fulfill the best performances and especially robustness and adaptive behavior under real conditions. Finally, using novel sources of information and novel signals, called signals of opportunity, represent novel areas of research and investigation. Therefore, Multi UAV-RFI detection and tracking under the LEO satellite sensors network have been considered as one of the most challenging and innovative problems to be solved in the last few decades. One of the strongest filtering algorithms that authors have developed and selected was the Gauss Hermite Quadrature filters package mixed with $H_\infty$ as a potential optimal multiple environment localization and tracking method.

Up to today, many real tests and data collections have been made available to perform different algorithms and benchmarks between different approaches. Very good positioning and promising results were obtained in stationary and dynamical modes performing with an error of several meters up to hundreds of meters.

## 7. Future Works

Based on the technical notes, observations and analysis made in this survey, it is important to select the best next move in this field with highly innovative impacts. Therefore, future possible directions to overcome RFI detection and tracking problems that may impact LEO SatCom and Global Navigation systems could be summarized in the following points:

- The development of new numerical methods and non-linear approximation (deterministic and stochastic) integration carrying out faster convergence and numerical stability especially for the geolocation of stationary RFI.
- The development of adaptive and learning monitoring of RFI signals parameters with simultaneous state and parameter learning algorithms, such as Gaussian processes, supervised and unsupervised techniques, etc.
- The development of machine learning and artificial intelligence algorithms such as: reinforcement learning and information reinforcement learning (based on information theoretical learning) with partial knowledge or full unknown models for RFI detection, identification and tracking.
- In addition, robust techniques such as the GHKF-H infinite presented and proposed should be optimized by using Fuzzy Logic for parameter tuning and other RL algorithms for best reactions to the environment uncertainty. To the best of our knowledge, this has not been done before in this field.
- Another issue is the development of real-time implementation of all these algorithms, such as defining and classifying the best performances in real-time and their respective feasibility.To achieve this kind of classification, it might be interesting to propose a computational time complexity for each algorithm for each case study: stationary target, dynamical target, maneuvering target, stationary sensors network, mobile sensors network, LEO satellite sensors network.
- More complex problems could be addressed by assuming multiple RFI-targets instead of only one, with multiple combinations of LEO satellite networks. The problem would be similar to multiple target tracking with only partial knowledge and uncertain data association algorithms to be developed.
- An original and interesting problem would be optimal sensors placement, or optimal constellation selection for optimizing RFI-targets detection and tracking using $H_\infty$ and Gauss Hermite Quadrature filters package algorithms to overcome high non-linearity degrees and sensor locations uncertainty.

In the end, an additional focus on highly accurate quadrature Kalman filters derived into stochastic forms could be the best next step to increase the accuracy of target state estimation, as well as the best estimate of RFI signals detected in the environment.

**Abbreviations**

| | |
|---|---|
| ADS-B | Automatic Dependent Surveillance-Broadcast |
| AEKF | Adaptive Extended Kalman Filter |
| AOA | Angle of Arrival |
| CAF | Cross Ambiguity Function |
| CAPITAL | Cellular Applied to IVHS Tracking and Location |
| CDFs | Cumulative Distribution Functions |
| CIR | Channel Impulse Response |
| CKF | Cubature Kalman Filter |
| CNN | Convolutional Neural Network |
| CRIAQ | Consortium for Research and Innovation in Aerospace in Quebec |
| CRLB | Cramér-Rao lower bound |
| CWLS | Constrained Weighted Least Square |
| DDR | Differential Doppler Rate |
| DL | Deep Learning |
| D-S | Dempster–Shafer |
| DVB | Digital Video Broadcasting |
| EKF | Extended Kalman Filter |
| EGNOS | European Geostationary Navigation Overlay Service |
| ÉTS | École de Technologie Supérieure |
| FDOA | Frequency Difference of Arrival |
| GA | Genetic Algorithm |
| GAGAN | GPS Aided Geo Augmented Navigation |
| GDOP | Geometric Dilution of Precision |
| GHKF | Gaussian Hermite Kalman Filter |
| GHQF | Gauss–Hermite Quadrature Filter |
| GLONASS | GLObal'naya NAvigatsioannaya Sputnikovaya Sistema |
| GMM | Gaussian Mixture Model |
| GMM-ITSF | Gaussian mixture measurement integrated track splitting filter |
| GMT | Ground Moving Targets |
| GNS | Navigation Systems |
| GNSS | Global Navigation Satellite Systems |
| GPS | Global Positioning System |
| GSN | GNSS Supervisory Authority |

| | |
|---|---|
| ICWLS | iterative constrained weighted least squares |
| INS | Inertial Navigation System |
| KF | Kalman Filtering |
| LASSENA | Laboratory of Space Technologies, Embedded System, Navigation and Avionic |
| LLS | Linear Least Squares |
| LOB | Line of Bearing |
| LOS | Line of Sigh |
| LS | Least Square |
| LSM | Least Square Methods |
| MAVs | Manned Aircraft Vehicles |
| ML | Maximum Likelihood |
| MLAT | Multilateration |
| MLE | Maximum Likelihood Estimator |
| MMF | multiple-model filter |
| MRPEs | mean relative position errors |
| MSPEs | mean square position errors |
| NLOS | Non-line of Sight |
| NLS | Non-linear Least Square |
| NSERC | Natural Sciences and Engineering Research Council of Canada |
| PDOA | Power Difference of Arrival |
| PF | Particle Filter |
| PNT | Positioning, Navigation, and Timing |
| QIKFs | Quadrature Information Kalman Filters |
| QKF | Quadrature Kalman filter |
| QLS | quadratic least squares |
| RFI | Radio-Frequency Interference |
| RMSE | Root Mean Square Error |
| RSS | Received Signal Strength |
| RTLS | Real-Time Locating System |
| SatCom | Satellite Communication |
| SBAS | Satellite Based Augmentation System |
| SDMC | System for Differential Correction and Monitoring |
| SDP | Semi-Definite Programming |
| SDR | Software-defined radios |
| SNR | Signal to the Noise ratio |
| SV | Space Vehicle |
| TDOA | Time Difference of Arrival |
| TLA | Tangent Linear Approximation |
| TOA | Time of Arrival |
| TS | Taylor Series |
| UAVs | Unmanned Aerial Vehicles |
| WAAS | Wide Area Augmentation System |
| WLS | Weighted Least Square |
| WSN | Wireless Sensor Networks |

## References

1. Kaiser, S.A.; Christianson, A.J.; Narayanan, R.M. Multistatic Doppler estimation using global positioning system passive coherent location. *IEEE Trans. Aerosp. Electron. Syst.* **2019**, *55*, 2978–2991. [CrossRef]
2. Liu, W.; Ding, J.; Zheng, J.; Chen, X.; Chih-Lin, I. Relay-Assisted Technology in Optical Wireless Communications: A Survey. *IEEE Access* **2020**, *8*, 194384–194409. [CrossRef]
3. Misra, D.; Misra, D.K.; Tripathi, S. Satellite communication advancement, issues, challenges and applications. *Int. J. Adv. Res. Comput. Commun. Eng.* **2013**, *2*, 1681–1686.
4. Gilski, P.; Stefański, J. Survey of radio navigation systems. *Int. J. Electron. Telecommun.* **2014**, *61*, 43–48. [CrossRef]
5. Morales-Ferre, R.; Richter, P.; Falletti, E.; de la Fuente, A.; Lohan, E.S. A survey on coping with intentional interference in satellite navigation for manned and unmanned aircraft. *IEEE Commun. Surv. Tutor.* **2019**, *22*, 249–291. [CrossRef]

6.  Carlo, D. GNSS Market Report Issue 5. Available online: http://www.gsa.europa.eu/gnss-market-report-issue-5-may-2017 (accessed on 1 May 2017).
7.  Jakhu, R.S. Satellites: Unintentional and Intentional Interference. In Proceedings of the Radio Frequency Interference and Space Sustainability, Washington, DC, USA, 17 June 2013.
8.  Wang, B.; Gan, X.; Liu, X.; Yu, B.; Jia, R.; Huang, L.; Jia, H. A novel weighted KNN algorithm based on RSS similarity and position distance for Wi-Fi fingerprint positioning. *IEEE Access* **2020**, *8*, 30591–30602. [CrossRef]
9.  Xiong, H.; Mai, Z.; Tang, J.; He, F. Robust GPS/INS/DVL navigation and positioning method using adaptive federated strong tracking filter based on weighted least square principle. *IEEE Access* **2019**, *7*, 26168–26178. [CrossRef]
10. Zhang, S.; Pan, X.; Mu, H. A multi-pedestrian cooperative navigation and positioning method based on UWB technology. In Proceedings of the 2020 IEEE International Conference on Artificial Intelligence and Information Systems (ICAIIS), Dalian, China, 20–22 March 2020; pp. 260–264.
11. Medina, D.A.; Romanovas, M.; Herrera-Pinzón, I.; Ziebold, R. Robust position and velocity estimation methods in integrated navigation systems for inland water applications. In Proceedings of the 2016 IEEE/ION Position, Location and Navigation Symposium (PLANS), Savannah, GA, USA, 11–16 April 2016; pp. 491–501.
12. Tahat, A.; Kaddoum, G.; Yousefi, S.; Valaee, S.; Gagnon, F. A Look at the Recent Wireless Positioning Techniques With a Focus on Algorithms for Moving Receivers. *IEEE Access* **2016**, *4*, 6652–6680. [CrossRef]
13. Gentile, C.; Alsindi, N.; Raulefs, R.; Teolis, C. *Geolocation Techniques: Principles and Applications*; Springer Science & Business Media: New York, NY, USA, 2012.
14. Wu, P.; Su, S.; Zuo, Z.; Guo, X.; Sun, B.; Wen, X. Time difference of arrival (TDoA) localization combining weighted least squares and firefly algorithm. *Sensors* **2019**, *19*, 2554. [CrossRef] [PubMed]
15. Noroozi, A.; Nayebi, M.M.; Amiri, R. Iterative constrained weighted least squares solution for target localization in distributed MIMO radar. In Proceedings of the 2019 27th Iranian Conference on Electrical Engineering (ICEE), Yazd, Iran, 30 April–2 May 2019; pp. 1710–1714.
16. Hao, W.; Wei-min, S.; Hong, G. A novel Taylor series method for source and receiver localization using TDOA and FDOA measurements with uncertain receiver positions. In Proceedings of the 2011 IEEE CIE International Conference on Radar, Chengdu, China, 24–17 October 2011; Volume 2, pp. 1037–1040.
17. Zhang, X.; Cui, Q.; Shi, Y.; Tao, X. Robust localisation algorithm for solving neighbour position ambiguity. *Electron. Lett.* **2013**, *49*, 1106–1107. [CrossRef]
18. Chui, C.K.; Chen, G. *Kalman Filtering*; Springer: Berlin/Heidelberg, Germany, 2017.
19. Pak, J.M.; Ahn, C.K.; Shmaliy, Y.S.; Lim, M.T. Improving reliability of particle filter-based localization in wireless sensor networks via hybrid particle/FIR filtering. *IEEE Trans. Ind. Inform.* **2015**, *11*, 1089–1098. [CrossRef]
20. Benzerrouk, H. *Modern Approaches in Nonlinear Filtering Theory Applied to Original Problems of Aerospace Integrated Navigation System with non-Gaussian Noise*; Saint Petersburg State University: Sankt-Peterburg, Russia, 2014.
21. Elgamoudi, A.; Benzerrouk, H.; Elango, G.A.; Landry, R. Gauss Hermite H∞ Filter for UAV Tracking Using LEO Satellites TDOA/FDOA Measurement—Part I. *IEEE Access* **2020**, *8*, 201428–201440. [CrossRef]
22. Zhao, J.; Mili, L. A theoretical framework of robust H-infinity unscented Kalman filter and its application to power system dynamic state estimation. *IEEE Trans. Signal Process.* **2019**, *67*, 2734–2746. [CrossRef]
23. Benzerrouk, H.; Nebylov, A.; Li, M. Multi-UAV Doppler information fusion for target tracking based on distributed high degrees information filters. *Aerospace* **2018**, *5*, 28. [CrossRef]
24. Benzerrouk, H.; Nebylov, A.; Salhi, H. Contribution in information signal processing for solving state space nonlinear estimation problems. *J. Signal Inf. Process.* **2013**, *4*, 375–384. [CrossRef]
25. Cao, Y.C.; Fang, J.A. Constrained Kalman filter for localization and tracking based on TDOA and DOA measurements. In Proceedings of the 2009 International Conference on Signal Processing Systems, Singapore, 15–17 May 2009; pp. 28–33.
26. del Peral-Rosado, J.A.; Seco-Granados, G.; Kim, S.; López-Salcedo, J.A. Network design for accurate vehicle localization. *IEEE Trans. Veh. Technol.* **2019**, *68*, 4316–4327. [CrossRef]
27. Wymeersch, H.; Seco-Granados, G.; Destino, G.; Dardari, D.; Tufvesson, F. 5G mmWave positioning for vehicular networks. *IEEE Wirel. Commun.* **2017**, *24*, 80–86. [CrossRef]
28. Gezici, S. A survey on wireless position estimation. *Wirel. Pers. Commun.* **2008**, *44*, 263–282. [CrossRef]
29. Sakpere, W.; Adeyeye-Oshin, M.; Mlitwa, N.B. A state-of-the-art survey of indoor positioning and navigation systems and technologies. *S. Afr. Comput. J.* **2017**, *29*, 145–197. [CrossRef]
30. Simon, D. *Optimal State Estimation: Kalman, H Infinity, and Nonlinear Approaches*; John Wiley & Sons: Hoboken, NJ, USA, 2006.
31. Wang, W.; Zhang, Y.; Tian, L. TOA-based NLOS error mitigation algorithm for 3D indoor localization. *China Commun.* **2020**, *17*, 63–72. [CrossRef]
32. Tsivgoulis, G. *Source Localization In Wireless Sensor Networks with Randomly Distributed Elements under Multipath Propagation Conditions*; Technical Report; Naval Postgraduate School: Monterey, CA, USA, 2009.
33. Fokin, G. TDOA Measurement Processing for Positioning in Non-Line-of-Sight Conditions. In Proceedings of the 2018 IEEE International Black Sea Conference on Communications and Networking (BlackSeaCom), Batumi, GA, USA, 4–7 June 2018; pp. 1–5.

34. Kim, J. Non-line-of-sight error mitigating algorithms for transmitter localization based on hybrid TOA/RSSI measurements. *Wirel. Netw.* **2020**, *26*, 3629–3635. [CrossRef]

35. Ho, T.J. Intelligent M-Robust Extended Kalman Filtering for Mobile Tracking. In Proceedings of the 2019 IEEE International Conference on Systems, Man and Cybernetics (SMC), Bari, Italy, 6–9 October 2019; pp. 2332–2337.

36. N de Sousa, M.; S Thomä, R. Enhancement of localization systems in NLOS urban scenario with multipath ray tracing fingerprints and machine learning. *Sensors* **2018**, *18*, 4073. [CrossRef] [PubMed]

37. Aghaie, N.; Tinati, M.A. Localization of WSN nodes based on NLOS identification using AOAs statistical information. In Proceedings of the 2016 24th Iranian Conference on Electrical Engineering (ICEE), Shiraz, Iran, 10–12 May 2016; pp. 496–501.

38. He, C.; Guo, F.; Li, X.; Zhang, M. Bias Analysis of AOA-Based Geolocation. In Proceedings of the 2018 2nd IEEE Advanced Information Management, Communicates, Electronic and Automation Control Conference (IMCEC), Xi'an, China, 25–27 May 2018; pp. 1711–1715.

39. Wang, Y.; Ho, K. An asymptotically efficient estimator in closed-form for 3-D AOA localization using a sensor network. *IEEE Trans. Wirel. Commun.* **2015**, *14*, 6524–6535. [CrossRef]

40. Choi, S.; Cha, J. Performance analysis of the jamming signal geolocation system using on-board AoA estimator mounted on UAV. In Proceedings of the 2017 17th International Conference on Control, Automation and Systems (ICCAS), Jeju, Korea, 18–21 October 2017; pp. 1976–1979.

41. Zheng, Y.; Sheng, M.; Liu, J.; Li, J. Exploiting AoA estimation accuracy for indoor localization: A weighted AoA-based approach. *IEEE Wirel. Commun. Lett.* **2018**, *8*, 65–68. [CrossRef]

42. Gezici, S.; Tian, Z.; Giannakis, G.B.; Kobayashi, H.; Molisch, A.F.; Poor, H.V.; Sahinoglu, Z. Localization via ultra-wideband radios: A look at positioning aspects for future sensor networks. *IEEE Signal Process. Mag.* **2005**, *22*, 70–84. [CrossRef]

43. Liang, K.; Huang, Z.; He, J. A passive localization method of single satellite using TOA sequence. In Proceedings of the 2016 2nd IEEE International Conference on Computer and Communications (ICCC), Chengdu, China, 14–17 October 2016; pp. 1795–1798.

44. Ho, K.; Lu, X.; Kovavisaruch, L.O. Source localization using TDOA and FDOA measurements in the presence of receiver location errors: Analysis and solution. *IEEE Trans. Signal Process.* **2007**, *55*, 684–696. [CrossRef]

45. Sun, Y.; Ho, K.; Wan, Q. Solution and analysis of TDOA localization of a near or distant source in closed form. *IEEE Trans. Signal Process.* **2018**, *67*, 320–335. [CrossRef]

46. Meng, Y.; Xu, J.; Huang, Y.; He, J. Key factors of multi-station TDOA passive location study. In Proceedings of the 2015 7th International Conference on Intelligent Human-Machine Systems and Cybernetics, Hangzhou, China, 26–27 August 2015; Volume 2, pp. 220–223.

47. Zhang, C.; Qin, N.; Xue, Y.; Yang, L. Received signal strength-based indoor localization using hierarchical classification. *Sensors* **2020**, *20*, 1067. [CrossRef] [PubMed]

48. Basar, E.; Di Renzo, M.; De Rosny, J.; Debbah, M.; Alouini, M.S.; Zhang, R. Wireless communications through reconfigurable intelligent surfaces. *IEEE Access* **2019**, *7*, 116753–116773. [CrossRef]

49. Ciuonzo, D.; Rossi, P.S.; Willett, P. Generalized Rao test for decentralized detection of an uncooperative target. *IEEE Signal Process. Lett.* **2017**, *24*, 678–682. [CrossRef]

50. Shoari, A.; Seyedi, A. Detection of a non-cooperative transmitter in Rayleigh fading with binary observations. In Proceedings of the MILCOM 2012—2012 IEEE Military Communications Conference, Orlando, FL, USA, 29 October–1 November 2012; pp. 1–5.

51. Blay, R.C.; Akos, D.M. GNSS RFI localization using a hybrid TDOA/PDOA approach. In Proceedings of the 2018 International Technical Meeting of The Institute of Navigation, Reston, VA, USA, 19 January 2018; pp. 703–712.

52. Tucker, J.A.; Puskar, C.; Lee, C.; Akos, D. GPS/GNSS Interference Power Difference of Arrival (PDOA) Localization Weighted via Nearest Neighbors. In Proceedings of the 33rd International Technical Meeting of the Satellite Division of The Institute of Navigation (ION GNSS+ 2020), Online, 21–25 September 2020; pp. 3550–3560.

53. Guo, S.; Jackson, B.; Wang, S.; Inkol, R.; Arnold, W. A novel density-based geolocation algorithm for a noncooperative radio emitter using power difference of arrival. In Proceedings of the SPIE Defense, Security, and Sensing, Orlando, FL, USA, 25–29 April 2011; Volume 8061, p. 80610E.

54. He, L.; Li, H.; Lu, M. Dual-antenna GNSS spoofing detection method based on Doppler frequency difference of arrival. *GPS Solut.* **2019**, *23*, 78. [CrossRef]

55. Broad, J.T.; Savage, L.M. Frequency Difference of Arrival (FDOA) for Geolocation. U.S. Patent 9,702,960, 11 July 2017.

56. Vesely, J. Differential doppler target position fix computing methods. In Proceedings of the International Conference on Circuits, Systems, Signals, San Francisco, CA, USA, 22–24 October 2019; pp. 284–287.

57. Landry, R.; Nguyen, A.; Rasaee, H.; Amrhar, A.; Fang, X.; Benzerrouk, H. Iridium Next LEO satellites as an alternative PNT in GNSS denied environments—Part 1. *Inside GNSS Mag.* **2019**, 56–64.

58. O'Donoughue, N. *Emitter Detection and Geolocation for Electronic Warfare*; Artech House: Norwood, MA, USA, 2019.

59. Zhao, Y.; Qi, W.; Liu, P.; Chen, L.; Lin, J. Accurate 3D localisation of mobile target using single station with AoA–TDoA measurements. *IET Radar Sonar Navig.* **2020**, *14*, 954–965. [CrossRef]

60. Aernouts, M.; BniLam, N.; Podevijn, N.; Plets, D.; Joseph, W.; Berkvens, R.; Weyn, M. Combining TDoA and AoA with a particle filter in an outdoor LoRaWAN network. In Proceedings of the 2020 IEEE/ION Position, Location and Navigation Symposium (PLANS), Portland, OR, USA, 20–23 April 2020; pp. 1060–1069.

61. Chen, H.; Ballal, T.; Saeed, N.; Alouini, M.S.; Al-Naffouri, T.Y. A Joint TDOA-PDOA Localization Approach Using Particle Swarm Optimization. *IEEE Wirel. Commun. Lett.* **2020**, *9*, 1240–1244. [CrossRef]

62. Kim, D.G.; Park, G.H.; Kim, H.N.; Park, J.O.; Park, Y.M.; Shin, W.H. Computationally efficient TDOA/FDOA estimation for unknown communication signals in electronic warfare systems. *IEEE Trans. Aerosp. Electron. Syst.* **2017**, *54*, 77–89. [CrossRef]

63. Akos, D.M.; Blay, R.; Shivaramaiah, N.C. Hybrid Interference Localization. U.S. Patent Application 16/246,177, 18 July 2019.

64. Zhao, Y.; Li, Z.; Hao, B.; Wan, P.; Wang, L. How to select the best sensors for TDOA and TDOA/AOA localization? *China Commun.* **2019**, *16*, 134–145.

65. Yin, S.; Chen, D.; Zhang, Q.; Liu, M.; Li, S. Mining spectrum usage data: A large-scale spectrum measurement study. *IEEE Trans. Mob. Comput.* **2012**, *11*, 1033–1046.

66. Zhao, Y.; Lung, C.H.; Lambadaris, I.; Goel, N. A hybrid location identification method in wireless AD Hoc/sensor networks. In Proceedings of the 2009 Tenth International Conference on Mobile Data Management: Systems, Services and Middleware, Taipei, Taiwan, 18–21 May 2009; pp. 465–473.

67. Yin, J.; Wan, Q.; Yang, S.; Ho, K. A simple and accurate TDOA-AOA localization method using two stations. *IEEE Signal Process. Lett.* **2015**, *23*, 144–148. [CrossRef]

68. Nur-A-Alam, M.; Haque, M.M. A least square approach for tdoa/aoa wireless location in wcdma system. In Proceedings of the 2008 11th International Conference on Computer and Information Technology, Nadi, Fiji, 8–10 December 2016; pp. 686–690.

69. Li, W.; Liu, P. 3D AOA/TDOA emitter location by integrated passive radar/GPS/INS systems. In Proceedings of the 2005 IEEE International Workshop on VLSI Design and Video Technology, Suzhou, China, 28–30 May 2005; pp. 121–124.

70. Overfield, J.; Biskaduros, Z.; Buehrer, R.M. Geolocation of MIMO signals using the cross ambiguity function and TDOA/FDOA. In Proceedings of the 2012 IEEE International Conference on Communications (ICC), Ottawa, ON, Canada, 10–15 June 2012; pp. 3648–3653.

71. Abbasbandy, S. Improving Newton–Raphson method for nonlinear equations by modified Adomian decomposition method. *Appl. Math. Comput.* **2003**, *145*, 887–893. [CrossRef]

72. Elgamoudi, A.; Shahzad, A.; Landry, R. Contribution to develop a generic hybrid technique of satellite system for RFI geolocation. In Proceedings of the 2017 14th International Bhurban Conference on Applied Sciences and Technology (IBCAST), Islamabad, Pakistan, 10–14 January 2017; pp. 764–771.

73. Yatrakis, C.L. Computing the Cross Ambiguity Function œ A Review. Ph.D. Thesis, State University of New York, New York, NY, USA, 2005.

74. Deng, B.; Sun, Z.B.; Peng, H.F.; Xiong, J.Y. Source localization using TDOA/FDOA/DFS measurements with erroneous sensor positions. In Proceedings of the 2016 CIE International Conference on Radar (RADAR), Guangzhou, China, 10–13 October 2016; pp. 1–4.

75. Liu, Z.; Hu, D.; Zhao, Y.; Zhao, Y. An algebraic method for moving source localization using TDOA, FDOA, and differential Doppler rate measurements with receiver location errors. *EURASIP J. Adv. Signal Process.* **2019**, *2019*, 25. [CrossRef]

76. Hu, D.; Luo, L.; Huang, D.; Chen, S. A Joint TDOA, FDOA and Doppler Rate Parameters Estimation Method and Its Performance Analysis. In Proceedings of the 2019 IEEE 21st International Conference on High Performance Computing and Communications; IEEE 17th International Conference on Smart City; IEEE 5th International Conference on Data Science and Systems (HPCC/SmartCity/DSS), Zhangjiajie, China, 10–12 August 2019; pp. 2482–2486.

77. Zekavat, R.; Buehrer, R.M. *Handbook of Position Location: Theory, Practice and Advances*; John Wiley & Sons: Hoboken, NJ, USA, 2011; Volume 27.

78. Series, S. *Comparison of Time-Difference-of-Arrival and Angle-of-Arrival Methods of Signal Geolocation*; ITU: Geneva, Switzerland, 2011.

79. Podevijn, N.; Plets, D.; Trogh, J.; Martens, L.; Suanet, P.; Hendrikse, K.; Joseph, W. TDoA-based outdoor positioning with tracking algorithm in a public LoRa network. *Wirel. Commun. Mob. Comput.* **2018**, *2018*. [CrossRef]

80. Li, X.; Deng, Z.D.; Rauchenstein, L.T.; Carlson, T.J. Contributed Review: Source-localization algorithms and applications using time of arrival and time difference of arrival measurements. *Rev. Sci. Instrum.* **2016**, *87*, 041502. [CrossRef]

81. Hu, D.; Chen, S.; Bai, H.; Zhao, C.; Luo, L. CRLB for joint estimation of TDOA, phase, FDOA, and Doppler rate. *J. Eng.* **2019**, *2019*, 7628–7631. [CrossRef]

82. Lu, J.; Yang, X. Taylor Series Localization Algorithm Based on Semi-definite Programming. In Proceedings of the International Conference on Artificial Intelligence and Security, New York, NY, USA, 26–28 July 2019; pp. 488–497.

83. Ren, J.; Chen, J.; Bai, W. A new localization algorithm based on Taylor series expansion for NLOS environment. *Cybern. Inf. Technol.* **2016**, *16*, 127–136. [CrossRef]

84. Rossi, R.J. *Mathematical Statistics: An Introduction to Likelihood Based Inference*; John Wiley & Sons: Hoboken, NJ, USA, 2018.

85. Jia, T.; Shen, X.; Wang, H. Multistatic sonar localization with a transmitter. *IEEE Access* **2019**, *7*, 111192–111203. [CrossRef]

86. Watanabe, F. Wireless Sensor Network Localization Using AoA Measurements with Two-Step Error Variance-Weighted Least Squares. *IEEE Access* **2021**, *9*, 10820–10828. [CrossRef]

87. Wang, Y. Linear least squares localization in sensor networks. *Eurasip J. Wirel. Commun. Netw.* **2015**, *2015*, 1–7. [CrossRef]

88. Dardari, D.; Falletti, E.; Luise, M. *Satellite and Terrestrial Radio Positioning Techniques: A Signal Processing Perspective*; Academic Press: Cambridge, MA, USA, 2012.

89.    Kang, S.; Kim, T.; Chung, W. Hybrid RSS/AOA Localization using Approximated Weighted Least Square in Wireless Sensor Networks. *Sensors* **2020**, *20*, 1159. [CrossRef] [PubMed]

90.    Wang, D.; Zhang, P.; Yang, Z.; Wei, F.; Wang, C. A novel estimator for TDOA and FDOA positioning of multiple disjoint sources in the presence of calibration emitters. *IEEE Access* **2019**, *8*, 1613–1643. [CrossRef]

91.    Cheung, K.W.; So, H.C. A multidimensional scaling framework for mobile location using time-of-arrival measurements. *IEEE Trans. Signal Process.* **2005**, *53*, 460–470. [CrossRef]

92.    Díez-González, J.; Álvarez, R.; González-Bárcena, D.; Sánchez-González, L.; Castejón-Limas, M.; Perez, H. Genetic algorithm approach to the 3D node localization in TDOA systems. *Sensors* **2019**, *19*, 3880. [CrossRef] [PubMed]

93.    Beynon, M.; Curry, B.; Morgan, P. The Dempster–Shafer theory of evidence: An alternative approach to multicriteria decision modelling. *Omega* **2000**, *28*, 37–50. [CrossRef]

94.    O'Shea, T.J.; Roy, T.; Clancy, T.C. Over-the-air deep learning based radio signal classification. *IEEE J. Sel. Top. Signal Process.* **2018**, *12*, 168–179. [CrossRef]

95.    Chang, Y.T.; Wu, C.L.; Cheng, H.C. The Enhanced Locating Performance of an Integrated Cross-Correlation and Genetic Algorithm for Radio Monitoring Systems. *Sensors* **2014**, *14*, 7541–7562. [CrossRef] [PubMed]

96.    Challa, S.; Koks, D. Bayesian and dempster-shafer fusion. *Sadhana* **2004**, *29*, 145–174. [CrossRef]

97.    Van Nguyen, T.; Jeong, Y.; Shin, H.; Win, M.Z. Machine learning for wideband localization. *IEEE J. Sel. Areas Commun.* **2015**, *33*, 1357–1380. [CrossRef]

98.    Schmidhuber, J. Deep learning in neural networks: An overview. *Neural Netw.* **2015**, *61*, 85–117. [CrossRef]

99.    Bengio, Y.; Courville, A.; Vincent, P. Representation learning: A review and new perspectives. *IEEE Trans. Pattern Anal. Mach. Intell.* **2013**, *35*, 1798–1828. [CrossRef]

100.   Niitsoo, A.; Edelhäußer, T.; Eberlein, E.; Hadaschik, N.; Mutschler, C. A deep learning approach to position estimation from channel impulse responses. *Sensors* **2019**, *19*, 1064. [CrossRef]

101.   Foy, W.H. Position-location solutions by Taylor-series estimation. *IEEE Trans. Aerosp. Electron. Syst.* **1976**, *AES-12*, 187–194. [CrossRef]

102.   Fu, S.; Li, Y.; Zhang, M.; Zong, K.; Cheng, L.; Wu, M. Ultra-wideband pose detection system for boom-type roadheader based on Caffery transform and Taylor series expansion. *Meas. Sci. Technol.* **2017**, *29*, 015101. [CrossRef]

103.   Mehboob, U.; Qadir, J.; Ali, S.; Vasilakos, A. Genetic algorithms in wireless networking: Techniques, applications, and issues. *Soft Comput.* **2016**, *20*, 2467–2501. [CrossRef]

104.   NIST. Engineering Statistics, Handbook. Available online: https://www.itl.nist.gov/div898/handbook/eda/section3/eda3652.htm (accessed on 18 January 2021).

105.   Pajares, A.; Blasco, X.; Herrero, J.M.; Reynoso-Meza, G. A multiobjective genetic algorithm for the localization of optimal and nearly optimal solutions which are potentially useful: NevMOGA. *Complexity* **2018**, *2018*, 1792420. [CrossRef]

106.   Yang, X.S. *Nature-Inspired Optimization Algorithms*; Academic Press: Cambridge, MA, USA, 2020.

107.   Kim, Y.; Bang, H. Introduction to Kalman filter and its applications. In *Introduction and Implementations of the Kalman Filter*; IntechOpen: London, UK, 2018.

108.   Pititeeraphab, Y.; Jusing, T.; Chotikunnan, P.; Thongpance, N.; Lekdee, W.; Teerasoradech, A. The effect of average filter for complementary filter and Kalman filter based on measurement angle. In Proceedings of the 2016 9th Biomedical Engineering International Conference (BMEiCON), Luang Prabang, Laos, 7–9 December 2016; pp. 1–4.

109.   Zhao, D.; Sun, J.; Gui, G. En-route Multilateration System Based on ADS-B and TDOA/AOA for Flight Surveillance Systems. In Proceedings of the 2020 IEEE 91st Vehicular Technology Conference (VTC2020-Spring), Antwerp, Begium, 25–28 May 2020; pp. 1–6.

110.   Kim, D.; Ha, J.; You, K. Adaptive extended Kalman filter based geolocation using TDOA/FDOA. *Int. J. Control Autom.* **2011**, *4*, 49–58.

111.   Fu, K.; Zhang, D.; Tang, P.; Tang, Z.; He, W. Adaptive extended Kalman filter for a red shift navigation system. In Proceedings of the 2015 34th Chinese Control Conference (CCC), Hangzhou, China, 28–30 July 2015; pp. 5194–5199.

112.   Chen, Y.M.; Tsai, C.L.; Fang, R.W. TDOA/FDOA mobile target localization and tracking with adaptive extended Kalman filter. In Proceedings of the 2017 International Conference on Control, Artificial Intelligence, Robotics & Optimization (ICCAIRO), Prague, Czech Republic, 22–17 May 2017; pp. 202–206.

113.   MathWork. Radar Tracking. Available online: https://www.mathworks.com/help/dsp/ug/radar-tracking.html (accessed on 18 April 2021).

114.   Arasaratnam, I.; Haykin, S.; Hurd, T.R. Cubature Kalman filtering for continuous-discrete systems: Theory and simulations. *IEEE Trans. Signal Process.* **2010**, *58*, 4977–4993. [CrossRef]

115.   Arasaratnam, I.; Haykin, S. Cubature kalman filters. *IEEE Trans. Autom. Control* **2009**, *54*, 1254–1269. [CrossRef]

116.   Benzerrouk, H.; Nebylov, A.; Salhi, H. Quadrotor UAV state estimation based on High-Degree Cubature Kalman filter. *IFAC-PapersOnLine* **2016**, *49*, 349–354. [CrossRef]

117.   Jin, S.; Huang, H.; Li, Y.; Ren, Y.; Wang, Y.; Zhong, R. An Improved Particle Filter Based Track-Before-Detect Method for Underwater Target Bearing Tracking. In Proceedings of the OCEANS 2019-Marseille, Marseille, France, 17–20 June 2019; pp. 1–5.

118. Mihaylova, L.; Angelova, D.; Honary, S.; Bull, D.R.; Canagarajah, C.N.; Ristic, B. Mobility tracking in cellular networks using particle filtering. *IEEE Trans. Wirel. Commun.* **2007**, *6*, 3589–3599. [CrossRef]
119. Del Moral, P. Nonlinear filtering: Interacting particle resolution. *C. R. L'Acad. Sci.-Ser. I-Math.* **1997**, *325*, 653–658. [CrossRef]
120. Cho, J.A.; Na, H.; Kim, S.; Ahn, C. Moving-target tracking based on particle filter with TDOA/FDOA measurements. *Etri J.* **2012**, *34*, 260–263. [CrossRef]
121. Reynolds, D.A. Gaussian Mixture Models. *Encycl. Biom.* **2009**, *741*, 659–663.
122. Okello, N.; Fletcher, F.; Musicki, D.; Ristic, B. Comparison of recursive algorithms for emitter localisation using TDOA measurements from a pair of UAVs. *IEEE Trans. Aerosp. Electron. Syst.* **2011**, *47*, 1723–1732. [CrossRef]
123. Arasaratnam, I.; Haykin, S. Square-root quadrature Kalman filtering. *IEEE Trans. Signal Process.* **2008**, *56*, 2589–2593. [CrossRef]
124. Closas, P.; Fernandez-Prades, C.; Vila-Valls, J. Multiple quadrature Kalman filtering. *IEEE Trans. Signal Process.* **2012**, *60*, 6125–6137. [CrossRef]
125. Zhao, J.; Mili, L. A decentralized H-infinity unscented Kalman filter for dynamic state estimation against uncertainties. *IEEE Trans. Smart Grid* **2018**, *10*, 4870–4880. [CrossRef]
126. Wang, Q.; Li, J.; Zhang, M.; Yang, C. H-infinity filter based particle filter for maneuvering target tracking. *Prog. Electromagn. Res.* **2011**, *30*, 103–116. [CrossRef]
127. Ting Goh, S.; Zekavat, S.; Abdelkhalik, O. An Introduction to Kalman Filtering Implementation for Localization and Tracking Applications. In *Handbook of Position Location: Theory, Practice, and Advances*, 2nd ed.; John Wiley & Sons: Hoboken, NJ, USA, 2018; pp. 143–195.
128. Jokić, I.; Zečević, Ž.; Krstajić, B. State-of-charge estimation of lithium-ion batteries using extended Kalman filter and unscented Kalman filter. In Proceedings of the 2018 23rd International Scientific-Professional Conference on Information Technology (IT), Žabljak, Montenegro, 19–24 February 2018; pp. 1–4.
129. Zhang, W.; Gu, W.; Chen, C.; Chowdhury, M.; Kavehrad, M. Gaussian mixture sigma-point particle filter for optical indoor navigation system. In Proceedings of the SPIE OPTO 2014, San Francisco, CA, USA, 1–6 February 2014; Volume 9007, p. 90070K.
130. Nguyen, T. *Gaussian Mixture Model Based Spatial Information Concept for Image Segmentation*; University of Windsor: Windsor, ON, Canada, 2011.
131. Ke, D.; Chung, C.; Sun, Y. A novel probabilistic optimal power flow model with uncertain wind power generation described by customized Gaussian mixture model. *IEEE Trans. Sustain. Energy* **2015**, *7*, 200–212. [CrossRef]
132. Arasaratnam, I.; Haykin, S.; Elliott, R.J. Discrete-time nonlinear filtering algorithms using Gauss–Hermite quadrature. *Proc. IEEE* **2007**, *95*, 953–977. [CrossRef]
133. Díez-González, J.; Álvarez, R.; Prieto-Fernández, N.; Perez, H. Local Wireless Sensor Networks Positioning Reliability Under Sensor Failure. *Sensors* **2020**, *20*, 1426. [CrossRef]
134. Ma, Y.; Wang, B.; Pei, S.; Zhang, Y.; Zhang, S.; Yu, J. An indoor localization method based on AOA and PDOA using virtual stations in multipath and NLOS environments for passive UHF RFID. *IEEE Access* **2018**, *6*, 31772–31782. [CrossRef]
135. Rahouma, K.H.; Mostafa, A.S. 3D Geolocation Approach for Moving RF Emitting Source Using Two Moving RF Sensors. In Proceedings of the International Conference on Advanced Machine Learning Technologies and Applications, Cairo, Egypt, 28–30 March 2019; pp. 746–757.
136. Khalaf-Allah, M. Performance Comparison of Closed-Form Least Squares Algorithms for Hyperbolic 3-D Positioning. *J. Sens. Actuator Netw.* **2020**, *9*, 2. [CrossRef]
137. Bottomley, G.E.; Cairns, D.A. Approximate Maximum Likelihood Radio Emitter Geolocation With Time-Varying Doppler. *IEEE Trans. Aerosp. Electron. Syst.* **2018**, *55*, 429–443. [CrossRef]
138. Qu, X.; Xie, L. Source localization by TDOA with random sensor position errors—Part I: Static sensors. In Proceedings of the 2012 15th International Conference on Information Fusion, Singapore, 9–12 July 2012; pp. 48–53.
139. Shi, W.; Wong, V.W. MDS-based localization algorithm for RFID systems. In Proceedings of the 2011 IEEE International Conference on Communications (ICC), Kyoto, Japan, 5–9 June 2011; pp. 1–6.
140. Deng, B.; Yang, L.; Sun, Z.B.; Peng, H.F. Geolocation of a known altitude target using tdoa and GROA in the presence of receiver location uncertainty. *Int. J. Antennas Propag.* **2016**, *2016*, 3293418. [CrossRef]
141. Ho, K.; Xu, W. An accurate algebraic solution for moving source location using TDOA and FDOA measurements. *IEEE Trans. Signal Process.* **2004**, *52*, 2453–2463. [CrossRef]
142. Zhang, B.; Hu, Y.; Wang, H.; Zhuang, Z. Underwater source localization using TDOA and FDOA measurements with unknown propagation speed and sensor parameter errors. *IEEE Access* **2018**, *6*, 36645–36661. [CrossRef]
143. Li, Y.; Hao, C.; Li, M.; He, L.; Li, P.; Wan, Q. Moving Target Tracking Using TDOA and FDOA Measurements from Two UAVs with Varying Baseline. *J. Phys. Conf. Ser.* **2019**, *1169*, 012013. [CrossRef]
144. Li, Y.; Zhao, Z. Passive tracking of underwater targets using dual observation stations. In Proceedings of the 2019 16th International Bhurban Conference on Applied Sciences and Technology (IBCAST), Islamabad, Pakistan, 8–12 January 2019; pp. 867–872.
145. Kaune, R. Performance analysis of passive emitter tracking using TDOA, AOA and FDOA measurements. In Proceedings of the INFORMATIK 2010, Leipzig, Germany, 27 September–1 October 2010.

146. Li, X.; Yang, L.; Mihaylova, L.; Guo, F.; Zhang, M. Enhanced GMM-based filtering with measurement update ordering and innovation-based pruning. In Proceedings of the 2018 21st International Conference on Information Fusion (FUSION), Cambridge, UK, 10–13 July 2018; pp. 2572–2579.

147. Zandian, R.; Witkowski, U. Evaluation of H-infinity Filter in Time Differential Localization Systems. In Proceedings of the 3rd KuVS/GI Expert Talk on Localization, Lübeck, Germany, 12–13 July 2018; pp. 21–23.

148. Osman, M.; Alonso, R.; Hammam, A.; Moreno, F.M.; Al-Kaff, A.; Hussein, A. Multisensor Fusion Localization using Extended $H_\infty$ Filter using Pre-filtered Sensors Measurements. In Proceedings of the 2019 IEEE Intelligent Vehicles Symposium (IV), Paris, France, 9–12 June 2019; pp. 1139–1144.

149. Benzerrouk, H.; Landry, R.; Nebylov, V.; Nebylov, A. Novel INS/GPS/Fisheye-Camera Loosely/Tightly Coupled Enhancing Robust Navigation in Dense Urban Environment. In Proceedings of the 2020 27th Saint Petersburg International Conference on Integrated Navigation Systems (ICINS), Saint Petersburg, Russia, 25–27 May 2020; pp. 1–8.

150. Benzerrouk, H.; Landry, R.; Nebylov, V.; Nebylov, A. Robust INS/GPS Coupled Navigation Based on Minimum Error Entropy Kalman Filtering. In Proceedings of the 2020 27th Saint Petersburg International Conference on Integrated Navigation Systems (ICINS), Saint Petersburg, Russia, 25–27 May 2020; pp. 1–4.

151. Peral-Rosado, D.; José, A.; Saloranta, J.; Destino, G.; López-Salcedo, J.A.; Seco-Granados, G. Methodology for simulating 5G and GNSS high-accuracy positioning. *Sensors* **2018**, *18*, 3220. [CrossRef] [PubMed]

152. Borio, D.; Li, H.; Closas, P. Huber's non-linearity for GNSS interference mitigation. *Sensors* **2018**, *18*, 2217. [CrossRef] [PubMed]

153. Li, M.; Nie, W.; Xu, T.; Rovira-Garcia, A.; Fang, Z.; Xu, G. Helmert variance component estimation for multi-gnss relative positioning. *Sensors* **2020**, *20*, 669. [CrossRef]

154. Min, H.; Wu, X.; Cheng, C.; Zhao, X. Kinematic and dynamic vehicle model-assisted global positioning method for autonomous vehicles with low-cost GPS/camera/in-vehicle sensors. *Sensors* **2019**, *19*, 5430. [CrossRef]

155. Sebastien Paris. Particle Filter for Robot Localization Using WiFi Measuremen. Available online: https://www.mathworks.com/matlabcentral/fileexchange/21149-particle-filter-for-robot-localization-using-wifi-measuremen (accessed on 8 June 2021).

156. Li, X.; Jiang, Z.; Ma, F.; Lv, H.; Yuan, Y.; Li, X. LEO precise orbit determination with inter-satellite links. *Remote Sens.* **2019**, *11*, 2117. [CrossRef]

157. Li, X.; Zhang, K.; Ma, F.; Zhang, W.; Zhang, Q.; Qin, Y.; Zhang, H.; Meng, Y.; Bian, L. Integrated precise orbit determination of multi-GNSS and large LEO constellations. *Remote Sens.* **2019**, *11*, 2514. [CrossRef]